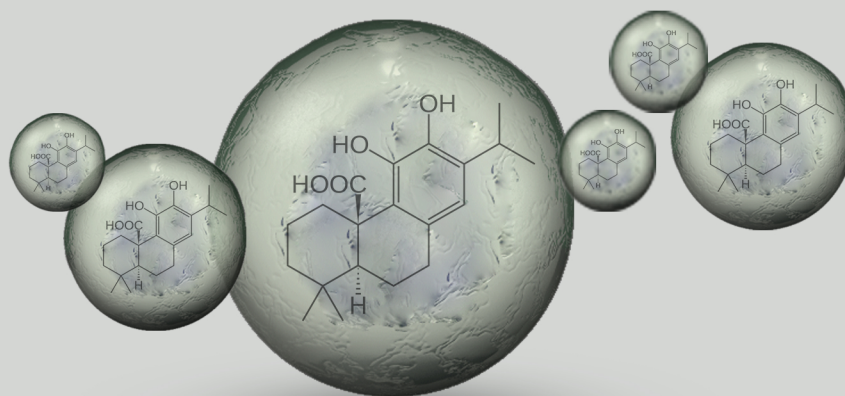


CARNOSIC ACID LOADED TPGS EMULSIFIED PLGA NANOPARTICLES: PREPARATION, PHYSICOCHEMICAL CHARACTERIZATION AND *IN VITRO* RELEASE STUDY

**THESIS SUBMITTED IN PARTIAL FULFILLMENT FOR THE REQUIREMENTS OF THE DEGREE OF
MASTER OF PHARMACY**



**SUBMITTED BY
MS. SANCHARI KARAK
ROLL NO. 001711402029
REGISTRATION NO. 140853 OF 2017-2018
EXAM ROLL NO. M4PHA19029**

**UNDER THE GUIDANCE OF
DR. SAIKAT DEWANJEE**

**DEPARTMENT OF PHARMACEUTICAL TECHNOLOGY
FACULTY OF ENGINEERING AND TECHNOLOGY
JADAVPUR UNIVERSITY
KOLKATA 700032, INDIA
2019**

**CARNOSIC ACID LOADED TPGS EMULSIFIED PLGA
NANOPARTICLES: PREPARATION, PHYSICOCHEMICAL
CHARACTERIZATION AND *IN VITRO* RELEASE STUDY**

THESIS SUBMITTED IN PARTIAL FULFILLMENT FOR THE REQUIREMENTS
OF THE DEGREE OF
MASTER OF PHARMACY

SUBMITTED BY
MS. SANCHARI KARAK
ROLL NUMBER- 001711402029
REGISTRATION NUMBER- 140853 OF 2017-2018
EXAMINATION ROLL NUMBER- M4PHA19029

UNDER THE GUIDANCE OF
DR. SAIKAT DEWANJEE

DEPARTMENT OF PHARMACEUTICAL TECHNOLOGY
FACULTY OF ENGINEERING AND TECHNOLOGY
JADAVPUR UNIVERSITY
KOLKATA 700032, INDIA
2019

Certificate of Approval

This is to certify that thesis entitled “**Carnosic acid loaded TPGS emulsified PLGA nanoparticles: preparation, physicochemical characterization and in vitro study**” has been carried out by Ms. Sanchari Karak under the supervision of Dr. Saikat Dewanjee, Assistant Professor, Department of Pharmaceutical Technology, Jadavpur University, Kolkata 700032. She has incorporated her findings into this thesis of the same title, being submitted by her, in partial fulfillment of the requirements for the degree of “Master of Pharmacy” of this university. She has pursued this work independently with proper care and attention to my entire satisfaction.

DR. SAIKAT DEWANJEE

Project supervisor
Department of Pharmaceutical technology
Faculty of Engineering and Technology
Jadavpur University
Kolkata 700032, India

PROF. PULOK K. MUKHERJEE

Head
Department of Pharmaceutical technology
Faculty of Engineering and Technology
Jadavpur University
Kolkata 700032, India

PROF. CHIRANJIB BHATTACHARJEE

Dean
Faculty of Engineering and Technology
Jadavpur University
Kolkata 700032, India

DECLARATION

I, the undersigned solemnly declare that the project report on “**Carnosic acid loaded TPGS emulsified PLGA nanoparticles: preparation, physicochemical characterization and in vitro study**” is submitted in the partial fulfillment of the requirements for the award of the degree of *Master of Pharmacy*, under the supervision of Dr. Saikat Dewanjee, Assistant Professor, Department of Pharmaceutical Technology, Jadavpur University, Kolkata 700032. I assert the statements made and conclusions drawn are an outcome of my research work. I further certify that the work contained in the report is original and has been done by me under the general supervision of my supervisor.

MS. SANCHARI KARAK

Roll no. 001711402029

Registration no. 140853 of 2017-2018

Examination roll no. M4PHA19029

Acknowledgements

*First and foremost, I would like to extend my sincere gratitude to my project supervisor, **Dr. Saikat Dewanjee**, Assistant Professor, Department of, Pharmaceutical Technology, Jadavpur University for sharing his pearls of wisdom and his dedicated help, advice, inspiration, encouragement, continuous support and endless guidance.*

*I wish to express my sincere gratitude to **Prof. Biswajit Mukherjee** Department of, Pharmaceutical Technology, Jadavpur University for his cordial supports throughout the course of my project.*

*I prefer to express my sincere appreciation to **Dr. Mita Chatterjee Debnath**, Infectious Diseases and Immunology Division, CSIR-Indian Institute of Chemical Biology, Kolkata, for her professional cooperation, thoughtful scientific input, and feedback during the course of my project.*

*I would like to thank **Prof. Pulok K. Mukherjee**, Head of the Department, Department of Pharmaceutical Technology, Jadavpur University for providing me the platform for implementation of my project.*

*I am thankful to my seniors **Dr. Raghuvir Gaonkar, Dr. Tarun Dua, Dr. Ranabir Sahu, Mr. Samrat Chakraborty, Ms. Swarnalata Joardar, Mr. Pratik Chakraborty, Mr. Chirantan Mukherjee, Mr. Ashique Al Hoque, Ms. Piu Das and Mr. Brahmachari Paul** for their guidance and moral support.*

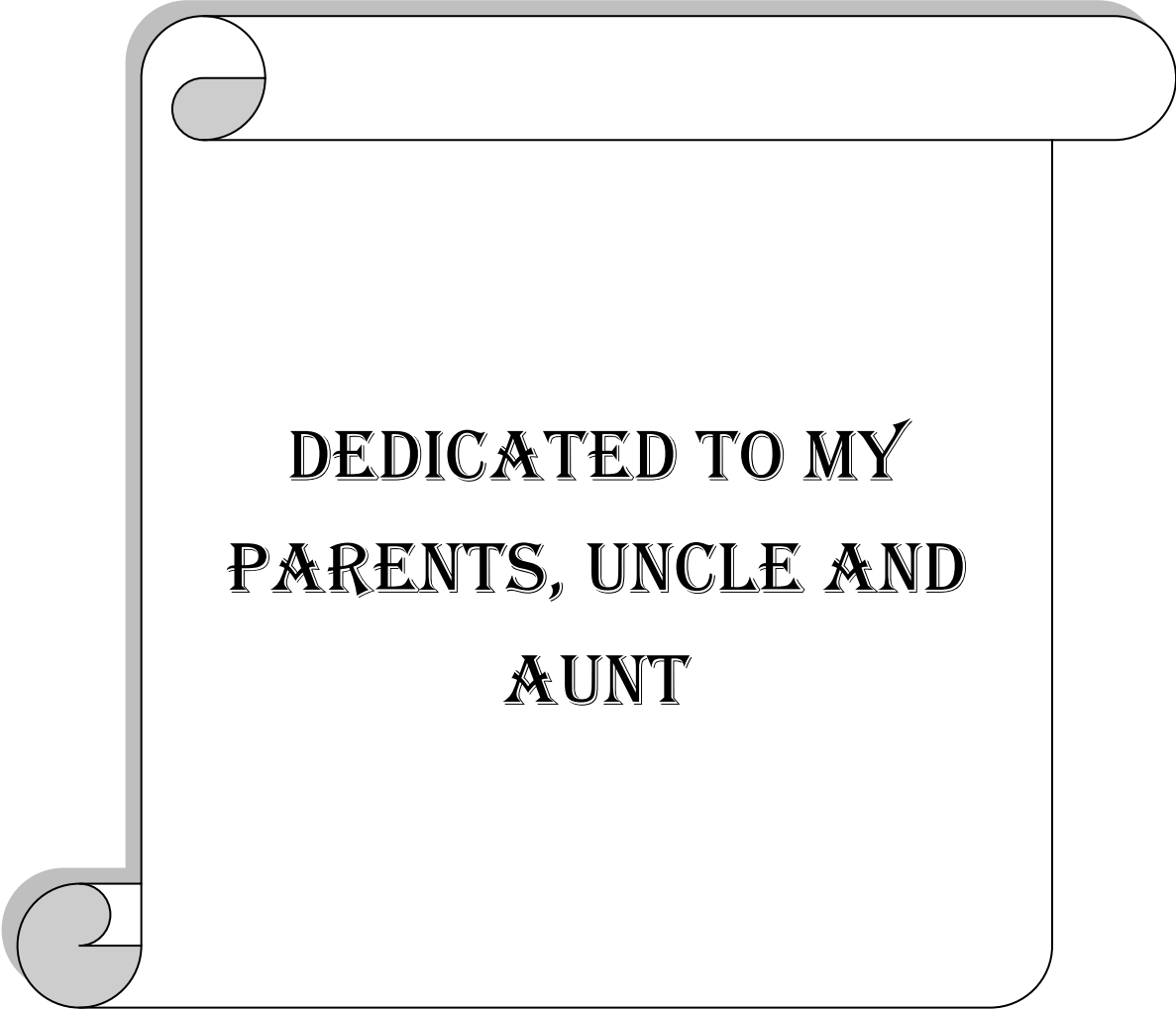
*I am also thankful to my peers **Susmita, Ajeya, Mohini, Deepayan, Shaunak and Sahajit**.*

*My acknowledgement will remain incomplete without mentioning the people who mean world to me, my grandmother **Mrs. Aloka Ghosh**; my parents, **Mr. Debasish Karak and Mrs. Kana Karak**; my uncle **Mr. Manoj Bali** and my aunt **Mrs. Mithu Bali**; my sisters **Madhura and Sanjana**; and my special friend **Rakesh**.*

Date:

Place:

(Sanchari Karak)



**DEDICATED TO MY
PARENTS, UNCLE AND
AUNT**

INDEX

Chapters	Contents	Page no
Chapter 1	Introduction	1-13
	1. Introduction	1
	1.1. Advantages of nanoparticle formulations	2
	1.2. Hazards associated with nanoparticles	3
	1.3. Classification of nanoparticles	4
	1.4. Applications of nanoparticles	6
	1.5. Methods of preparation of nanoparticles	8
	1.6. Characterization of nanoparticles	10
	1.7. Objective of study	13
Chapter 2	Literature review	14-27
	2. Literature review	14
	2.1. Literature review of CA	14
	2.2. Literature review of PLGA	17
	2.3. Literature review of TPGS	23
	2.4. Literature review on success of nanoparticle formulation	24
	2.5. Literature review on nanoprecipitation method	26
Chapter 3	Materials and methods	28-33
	3.1. Materials	28
	3.2. Methods	28
	3.2.1. Preparation of CA loaded nanoparticles	28
	3.2.2. Determination of λ_{\max} of CA	30
	3.2.3. Plotting standard curve of CA in ethyl acetate	30
	3.2.4. Characterisation of nanoparticles	30
	3.2.5. <i>In vitro</i> drug release study	32
Chapter 4	Results and discussion	34-50
	4.1. λ_{\max} of CA	34
	4.2. Standard curve of CA in ethyl acetate	34
	4.3. $^1\text{H-NMR}$	35
	4.4. FTIR	36
	4.5. Thermal analysis by DSC	39
	4.6. Crystallinity evaluation by XRD	41

4.7. NY, DL and EE	42
4.8. TEM	44
4.9. AFM	45
4.10. DLS	46
4.11. Surface Charge	47
4.12. Standard curve of CA in PBS	48
4.13. <i>In vitro</i> drug release study	49
Chapter 5 Conclusion	51
References	52-65

FIGURE CAPTIONS

Figures	Titles	Page no
Figure 1.1.	Nanoparticles.	1
Figure 1.2.	Different types of nanoparticles. Dendrimers (A), micelles (B), carbon nanotubes (C), metallic nanoparticles (D), polymeric nanoparticle (E) and polymer-drug conjugate (F).	4
Figure 1.3.	Different anticancer approaches of nanoparticles.	7
Figure 2.1.	Structure of CA.	14
Figure 2.2.	Major sources of CA. Leaves of <i>Rosmarinus officinalis</i> (a), <i>Salvia officinalis</i> (b) and <i>Origanum vulgare</i> (c).	15
Figure 2.3.	CA cures several complications.	16
Figure 2.4.	Structure of PLGA.	18
Figure 2.5.	Formation of PLGA from lactic acid and glycolic acid monomer	19
Figure 2.6.	Drug release from PLGA nanoparticles.	20
Figure 2.7.	Structure of TPGS.	23
Figure 3.1.	A schematic overview of CA nanoparticle preparation method.	29
Figure 4.1.	λ_{\max} of CA.	34
Figure 4.2.	Standard curve of CA in ethyl acetate.	35
Figure 4.3.	¹ H-NMR spectra of CA (a), PLGA (b), and CA-PLGA (c) mixture in CDCl ₃ .	37
Figure 4.4.	FTIR of CA (a), PLGA (b), TPGS (c), CA-PLGA-TPGS mixture (d), CA nanoparticles (e)	38
Figure 4.5.	DSC thermogram of CA (a), PLGA (b), CA-PLGA mixture (c), and CA nanoparticles (d).	40
Figure 4.6.	XRD of CA (a), PLGA (b), CA-PLGA (c), and CA nanoparticles (d).	42
Figure 4.7.	Comparison between NY, DL, and EE in different drug-polymer ratio.	44

Figure 4.8.	TEM image of CA nanoparticles.	45
Figure 4.9.	AFM image of CA nanoparticle: Three-dimensional view (a), topographical image (b) and surface height and length profile.	46
Figure 4.10.	Particle size distribution pattern of CA nanoparticles.	47
Figure 4.11.	Zeta potential distribution profile of CA nanoparticles.	48
Figure 4.12.	Standard curve of CA in PBS.	49
Figure 4.13.	Cumulative percent drug release of <i>in vitro</i> drug release of CA nanoparticles.	50

TABLE CAPTIONS

Tables	Titles	Page no
Table 3.1.	Amounts of drug and polymer used in nanoparticle formulation.	30
Table 4.1.	Endothermic peak temperatures of different components.	39
Table 4.2.	Highest intensity values of different components.	41
Table 4.3.	NY, DL and EE percentages of different drug-polymer ratio.	43

Chapter 1

Introduction

Contents

1. Introduction
 - 1.1. Advantages of nanoparticle formulations
 - 1.2. Hazards associated with nanoparticles
 - 1.3. Classification of nanoparticles
 - 1.4. Applications of nanoparticles
 - 1.5. Methods of nanoparticle preparation
 - 1.6. Characterization of nanoparticles
 - 1.7. Objective of study

1. Introduction

Carnosic acid (CA) is a natural diterpenoid compound belonging to benzenediol abietane group (Guerrero *et al.*, 2006). It is known to possess a number of therapeutic activities such as pro-apoptotic, antiproliferative, chemoprotective, antitumour, and antiplatelet effects (Nabekura *et al.*, 2010). Herein we report the formulation of CA enloaded Poly lactic-co-glycolic acid (PLGA) nanoparticles using vitamin E TPGS (d- α -tocopheryl polyethylene glycol succinate) as an emulsifier by nanoprecipitation method and determine size, surface morphology, surface charge, phycochemical characteristics, encapsulation efficiency and *in vitro* drug release profile.

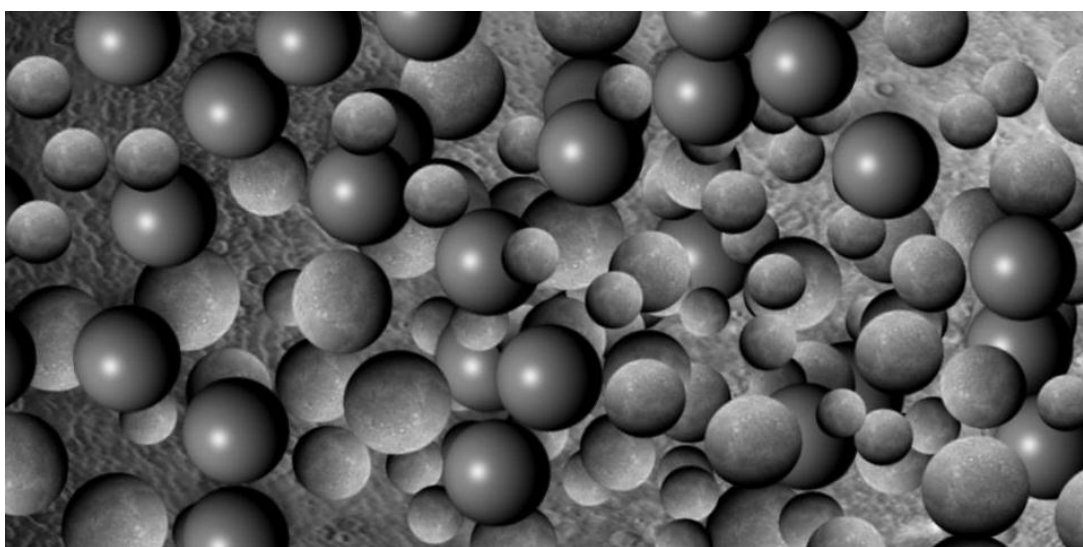


Figure 1.1. Nanoparticles

Pharmaceutical nanotechnology is an important milestone in the development of drug delivery system (Saini *et al.*, 2010). Pharmaceutical nanoparticles (Figure 1.1.) are defined as solid, nano-sized (< 100 nm in diameter) drug carrier that are biocompatible as well as biodegradable (Pal *et al.*, 2011). The nanospheres and nanocapsules togetherly termed as nanoparticles. In nanosphere matrix system drug is uniformly dispersed, on the other hand in nanocapsule system drug is enclosed in unique polymeric outerlayer (Guterres *et al.*, 2007). This novel drug delivery system is much more acceptable to overcome the problems regarding conventional drug delivery systems in terms of improved stability, improved bioavailability, increased drug loading, ability of controlled release, possibility to use in different routes of administration, improved therapeutic efficacy, prolonged circulation, reduced side effects, and the capability to deliver both hydrophilic and hydrophobic drug molecules

(Singh & Lillard, 2009). Not only drug delivery, nanomedicines are also being used for diagnostic purposes also (Jia, 2005).

1.1. Advantages of nanoparticle formulations

1.1.1. Increased solubility and dissolution rate of drug

The nanoparticles provide huge effective surface area due to their smaller size, which in turn leads to the high concentration gradient of poorly soluble compounds, controlled pharmacokinetic properties and increased dissolution rate of the incorporated drug component. Therefore, the particle size in turn makes the nanoparticles highly soluble for both hydrophilic and hydrophobic drugs (Hu *et al.*, 2004). The hydrophobic drugs which are poorly bioavailable, when applied by conventional drug delivery method, can achieve higher degree of bioavailability being incorporated in the nanoparticles (Hu *et al.*, 2004).

1.1.2. Increased oral bioavailability

Aqueous nanosuspensions offer higher systemic exposure and rapid achievement of peak plasma concentrations than other conventional oral formulations, with median time to maximum drug concentration, as the nanoparticles have higher solubility in the systemic circulation than free drug (Morgen *et al.*, 2012). It was also reported that nanoparticles can improve the oral bioavailability of both hydrophobic and hydrophilic drugs (Jial, 2005). Being biodegradable, erosion of nanoparticles release the drug for long time which provides increased bioavailability (Morgen *et al.*, 2012).

1.1.3. Long duration of action

The contribution of nanoparticles in interaction with the targeted tissues as well as cells, which permits improved lipid-lipid exchange with the lipid monolayer of the nanoparticles (Guzman *et al.*, 1996). This property of nanoparticle serves as drug depots, which exhibits prolonged release kinetics and long persistence at the target site (Guzman *et al.*, 1996).

1.1.4. Targeted drug delivery

Nanoparticles provide targeted drug delivery to the organs, tissues and cells, which simultaneously reduces toxic effects (Moghimi *et al.*, 2001). It may be active or passive kind of targeted delivery. In active targeting, the therapeutic agent is conjugated to a tissue or cell-specific ligand (Lamprecht *et al.*, 2001). In passive targeting incorporation of the therapeutic agent into a macromolecule or nanoparticle takes place, which passively reaches the target organ, where drugs encapsulated in nanoparticles or drugs coupled to macromolecules can passively target tumors (Sahoo

et al., 2002). Moreover, as it is capable to penetrate blood-brain-barrier, the delivery of antitumor drugs encapsulated in nanoparticles is a reliable way to carry drugs in the central nervous system (Singh & Lillard, 2009).

1.2. Hazards associated with nanoparticles

Polymeric nanoparticles are being used in medical applications in large number due to their high biological safety, biodegradability, easy production method and modification of the drug delivery system. PLGA polymer is highly used in the preparation of nanoparticles, microspheres, pellets, and microcapsules. It was reported that drugs encapsulated in PLGA are effective to reduce adverse effects and they use to accumulate in tumor cells (Han *et al.*, 2018). But it has been also reported that the consequences like toxicity of the respiratory system, dysfunction of systemic circulation, oxidative stress, and disruption of the endocrine system may take place on prolonged use (Som *et al.*, 2013). Nanoparticles have been found to cause formation of the reactive oxygen species, which further leads to oxidative damages, either directly through catalyzing free radical reactions or indirectly by leading to interference with cellular homeostasis (Yan *et al.*, 2013). The presence of the reactive oxygen species may even lead to damage to several organelles, such as the endoplasmic reticulum (Chen *et al.*, 2014). Beside inducing reactive oxygen species polymeric nanoparticles can also sensitize the cells to other forms of stress (Zhang *et al.*, 2012). As the result of the cellular damage by these polymeric nanoparticles, they can induce different types of pathways of programmed cell death, including apoptosis, regulated necrosis and autophagic cell death on prolonged use (Andon & Fadeel, 2013).

1.3. Classification of nanoparticles

Nanoparticles intended for drug delivery, diagnostic and other clinical uses are of various types (Figure 1.2.) based on their structure and different purposes; these include dendrimers, micelles, carbon nanotubes, metallic nanoparticles, polymeric nanoparticles, polymer-drug conjugate etc. (Onoue *et al.*, 2014).

1.3.1. Dendrimers

Dendrimers (as shown in Figure 1.2.A) are preferred for therapeutic approaches, as these can enhance the water solubility, bioavailability, and biocompatibility of drugs, which have poor solubility in water and can be applied through different routes of drug administration successfully. Besides, these provide the delivery of the drug to the targeted organ or cell and provide desired therapeutic effect (Yavuz *et al.*, 2013).

1.3.2. Micelles

The physicochemical nature of the micelles (as shown in Figure 1.2.B) also termed as nanomicelles consisting of a hydrophobic core and a hydrophilic outer layer, renders these spherical vesicles highly acceptable for passive drug delivery of hydrophobic compounds. Core cross-linked polymeric micelles have evolved as a promising strategy to prevent the premature disintegration and release of therapeutic component (Mandal *et al.*, 2017).

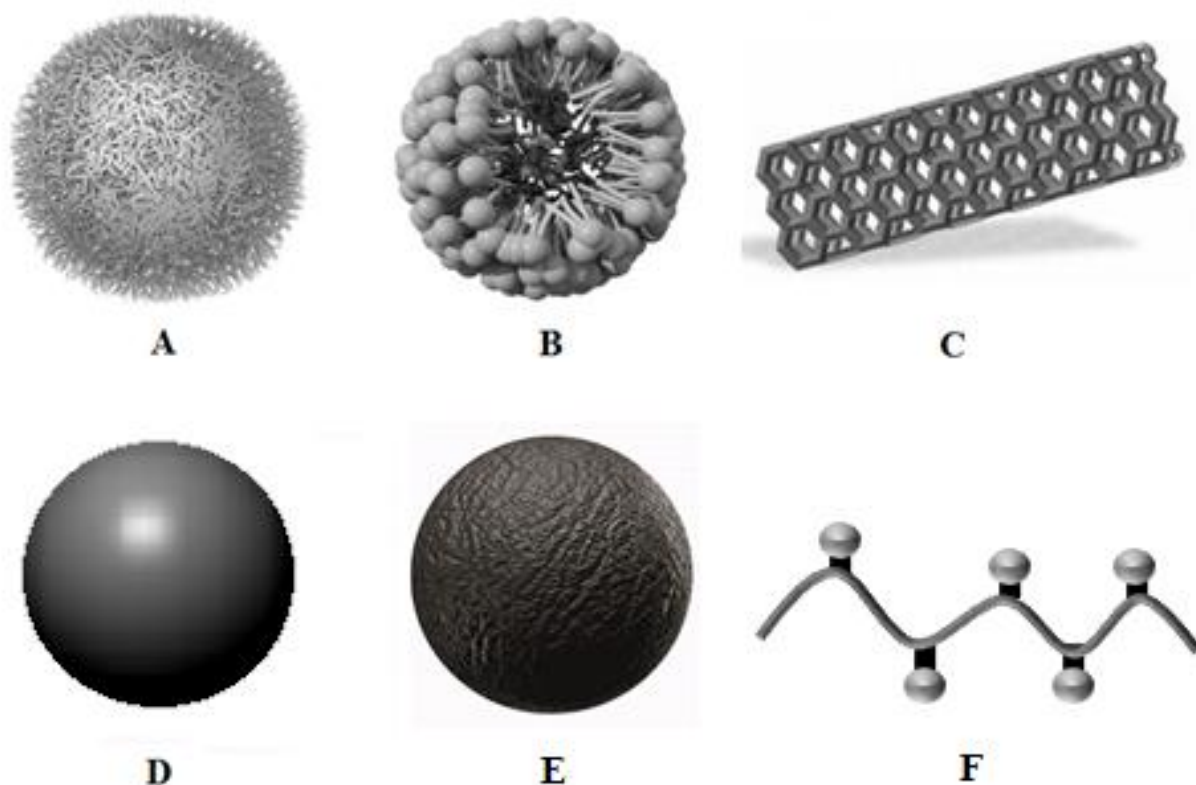


Figure 1.2. Different types of nanoparticles. Dendrimers (A), micelles (B), carbon nanotubes (C), metallic nanoparticles (D), polymeric nanoparticle (E) and polymer-drug conjugate (F).

1.3.3. Carbon nanotubes

After discovery of carbon nanotubes (as shown in Figure 1.2.C) in 1991 their acceptability in the field of drug delivery gradually increased as they have attracted attention on account to their outstanding structural, electro-mechanical properties, large surface area, thermal stability, and metallic-to-semiconducting current carrying capacity (Karimi *et al.*, 2015). These are used to in hthe purpose of delivering peptides, nucleic acids, and drug molecules (McDevitt *et al.*, 2007).

1.3.4. Metallic nanoparticles

Metallic nanoparticles (as shown in Figure 1.2.D) are now rising as good delivery carrier for drugs; many anticancer drugs are reported to be delivered to the targeted site enloaded in metallic nanoparticles (McDevitt *et al.*, 2007). For the preparation of metallic nanoparticles different metals have been used though silver and gold nanoparticles are the primary choice for therapeutic and diagnostic uses (McDevitt *et al.*, 2007). Surface functionalization on metallic nanonarticles is easy to do and different ligands have been conjugated on the surface. Diversity of ligands such as sugars, peptide, protein and DNA has been linked to nanoparticles (McDevitt *et al.*, 2007).

1.3.5. Polymeric nanoparticles

Polymeric nanoparticles (as shown in Figure 1.2.E) are highly being used in delivery of anticancer drugs (Kamaly *et al.*, 2016). For example, PLGA can be used for the entrapment of most types of therapeutics with a wide range of molecular weights, such PLGA is available in varrying ratios of glycolic acid and lactic acid monomer unit, and can be made-up into particles of different sizes and shapes (Kamaly *et al.*, 2016). Synthetic and semisynthetic polymers are a very potential media for nanoparticle based drug delivery as they provide a plethora of advantages like increased efficacy, lower toxicity, controlled release rates, sustained bioactivity, manufacturing reproducibility, higher stability, lesser administration frequency and capability of codelivering drugs resulting in synergistic effects. Examples of some commonly used polymers for preparing nanoparticles intended for drug delivery are poly (lactic acid) [PLA], poly (lactic-co-glycolic acid) [PLGA], poly (ethylene glycol-co- (lactic-glycolic acid)), poly (methyl) methacrylate, poly (caprolactone) and poly (alkyl) cyanoacrylates. These polymeric nanoparticles are often produced by pairing with polyethylene glycol to provide prolonged systemic circulation time (McDevitt *et al.*, 2007).

1.3.6. Polymer drug conjugate

Polymer drug conjugates (as shown in Figure 1.2.F) are prepared by the conjugating low molecular weight drugs with the biodegradable polymers (Makadia *et al.*, 2011). It differs from the polymeric nanoparticles, as the drug is not incorporated inside any polymeric shell, but only physically adhered with polymeric chain (Makadia *et al.*, 2011). This interaction or conjugation between drug and polymer chain causes vast change in pharmacokinetic disposition of drug in the organs as well as in the cells

(Makadia *et al.*, 2011). They are prepared to increase the overall molecular weight, which enhances their retention in cancer cells through enhanced permeation and retention effect using passive delivery approach (Makadia *et al.*, 2011).

1.4. Applications of nanoparticles

1.4.1. Drug delivery

Use of nanoparticles in drug delivery purpose is highly acceptable due to the targeted delivery even in cellular levels (Tao *et al.*, 2014). In this less amount of drug is required due to higher bioavailability, smaller amount of drug usage also reduces toxicity (Nahar *et al.*, 2006). This highly selective approach can reduce costs and pain to the patients (Nahar *et al.*, 2006). A large variety of nanoparticles such as dendrimers and polymeric nanoparticles find application (Nahar *et al.*, 2006). Micelles obtained from block co-polymers, are used for drug encapsulation. Micelles transport small drug molecules to the desired location (Tao *et al.*, 2014). Iron nano particles or gold nanoparticles are found to be important in the cancer treatment (Tao *et al.*, 2014). The pharmacological and therapeutic properties of drugs can be enhanced by using lipid and polymer based nanoparticles (Tao *et al.*, 2014).

1.4.2. Protein and peptide delivery

Protein and peptides are macromolecular biopharmaceuticals (Takeuchi *et al.*, 2001). They have therapeutic activities against various diseases and disorders as they exercise multiple biological actions in human body (Takeuchi *et al.*, 2001). But due to large structure they struggle to permeate cell membrane. Applications of nanoparticles were found to be useful in delivering the myelin antigens, which induce immune tolerance in a mouse model with relapsing multiple sclerosis (Takeuchi *et al.*, 2001).

1.4.3. Anticancer approaches

The enhanced permeability and retention effect of nanoparticles raise their acceptability in the area of the tumor targets (Gao *et al.*, 2004). This site specific delivery can also be achieved by active targeting with the help of ligands on the surface layer of nanoparticles (Gao *et al.*, 2004). Nanoparticles have the unique quality to restrict the drug distribution to the particular target organ (Gao *et al.*, 2004). Targeted drug delivery reduces the drug exposure to the normal and healthy cells. A report claims that mice treated with doxorubicin enloaded poly (isohexylcyanoacrylate) nanopsheres exhibited higher concentrations of doxorubicin in the liver, spleen and lungs than in mice treated with free doxorubicin drug (Gao *et*

al., 2004). It was also reported that polymeric nanoparticles possess favourable qualities such as biodegradation; biodegradability; safety and high aqueous solubility, along with the entrapment efficiency of the drugs having poor water solubility have a great influence on the drug distribution pattern *in vivo* (Gao *et al.*, 2004). Nanoparticles are helpful due to their rapid dissolution rate, within 30min to 3 h (Gao *et al.*, 2004).

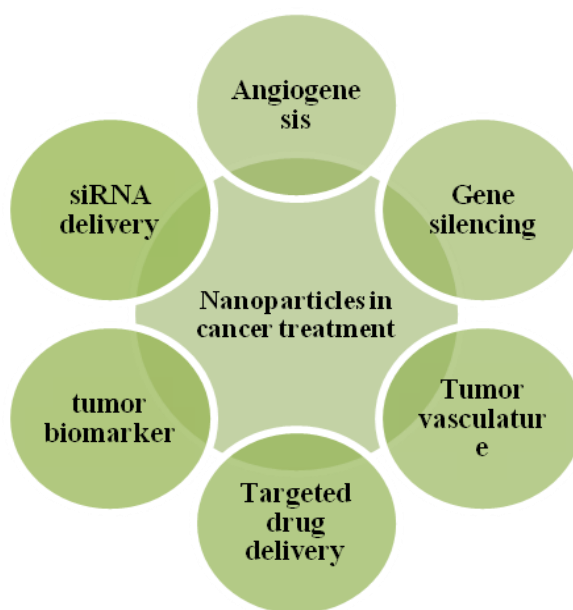


Figure 1.3. Different anticancer approaches of nanoparticles.

Highly selective therapy for cancer therapy is required where tumor cells will be the specific target (Nabekura *et al.*, 2010). Angiogenesis, gene silencing, tumor vasculature, targeted drug delivery, tumor biomarking, small interfering ribonucleic acid (siRNA) are the basis of nanoparticle based anticancer therapy. It was reported that paramagnetic nanoparticles, quantum dots, nanoshells and nanosomes are widely used for cancer diagnostic purposes (Tao *et al.*, 2014). Carbon nanotubes are proved to be effective in breast cancer, where gene silencing has been done with small the nanotubes interfering RNA (Karimi *et al.*, 2015). Another report proved that quantum dots are fruitful in prostate cancer, according to the experiments on mice (Kwon *et al.*, 2013). Being hydrophobic Paclitaxel has poor bioavailability. Albumin-coated paclitaxel was approved by the FDA in 2005 for metastatic breast cancer treatment and exhibited good efficacy against advanced pancreatic cancer. Nanospheres enloaded with albumin-coated paclitaxel can be used to transport insoluble drug (Guarneri *et al.*, 2012).

1.4.4. Application in neurodegenerative diseases

One of the most important applications of nanoparticles in the field of pharmacy is in the treatment of neuro degenerative disorders (Torres-Ortega *et al.*, 2019). To deliver drugs for central nervous system, different nanoparticles such as, dendrimers, nanogels, nanoemulsions, liposomes, polymeric nanoparticles, solid lipid nanoparticles, and nano suspensions have been studied (Torres-Ortega *et al.*, 2019). These nanoparticles have ability to cross blood-brain-barrier by endocytosis or transcytosis. Nanoparticles are found to be effective Alzheimer's disease, brain tumors, HIV encephalopathy and acute ischemic stroke (Torres-Ortega *et al.*, 2019).

1.4.5. Application in ophthalmology

Nanoparticles are used in treatment of oxidative stress and determination of intraocular pressure (Diebold *et al.*, 2010). Scars appear after glaucoma surgery can be prevented by nanoparticles and for treatment of retinal degenerative disease using gene therapy; prosthetics; and regenerative nano medicine; various nanoparticulate systems like microemulsions, nanosuspensions, nanoparticles, liposomes, niosomes, dendrimers and cyclodextrins in the field of ocular drug delivery and also depicts how the various upcoming of nanotechnology like nanodiagnostics, nanoimaging and nanomedicine can be utilized to explore the frontiers of ocular drug delivery and therapy (Diebold *et al.*, 2010). A novel nano scale dispersed eye ointment for the treatment of severe evaporative dry eye has been successfully developed, in which ointment petrolatum and lanolin were used as semisolid lipids (Diebold *et al.*, 2010).

1.5. Methods of preparation of nanoparticles

1.5.1. Emulsion-solvent evaporation method

In this process, initially the emulsification of the polymer solution into an aqueous phase is done (Jaiswal *et al.*, 2004). Then polymer solvent is then evaporated to induce the precipitation as nanospheres (Jaiswal *et al.*, 2004). The nanoparticles are collected by ultracentrifugation and washed with distilled water to remove undesired residues (Jaiswal *et al.*, 2004).

1.5.2. Double emulsion and evaporation method

Double emulsion and evaporation method helps to avoid the issue of poor entrapment of hydrophilic drugs (El-shabouri *et al.*, 2002). In this method, aqueous drug solution is added to the organic polymer solution with vigorous stirring to form w/o emulsions (El-shabouri *et al.*, 2002). This w/o emulsion is added into a second aqueous phase with continuous stirring to form the w/o/w emulsion (El-shabouri *et al.*, 2002). The

emulsion is then subjected to solvent removal by evaporation and nanoparticles can be isolated by centrifugation at high speed (El-shabouri *et al.*, 2002). The formulated nanoparticles must be thoroughly washed before lyophilisation (El-shabouri *et al.*, 2002).

1.5.3. Salting out method

This method is based on the separation of a water-miscible solvent from aqueous solution by salting-out effect (Takeuchi *et al.*, 2001). After dissolving polymer and drug in a solvent, it is emulsified into an aqueous gel containing the salting out agents, such as electrolytes namely magnesium chloride, calcium chloride etc. or non-electrolytes viz. as sucrose and a colloidal stabilizer such as polyvinylpyrrolidone or hydroxyethylcellulose (Takeuchi *et al.*, 2001). This oil/water emulsion is then diluted with a sufficient volume of water or in aqueous system to enhance the diffusion of solvent into the aqueous phase, which induces the formation of nanospheres (Takeuchi *et al.*, 2001).

1.5.4. Emulsion diffusion method

In emulsion diffusion method, an encapsulating polymer is dissolved in a partially water-miscible solvent, such as propylene carbonate, benzyl alcohol etc. and is saturated with water to ensure the initial thermodynamic equilibrium of both the liquids (El-shabouri *et al.*, 2002). Then the polymer-water saturated solvent phase is emulsified in an aqueous solution containing stabilizer leading to the solvent diffusion to the external phase. The nanospheres or nanocapsules are formed in accordance to the oil to polymer ratio (El-shabouri *et al.*, 2002). Finally, the solvent is eliminated by evaporation or filtration, according to its boiling point (El-shabouri *et al.*, 2002).

1.5.5. Solvent displacement or precipitation method

Solvent displacement or precipitation method involves the precipitation of a preformed polymer from an organic solution and the diffusion of the organic solvent into the aqueous medium in the presence or absence of surfactant (Pal *et al.*, 2011). Polymers and drugs are dissolved in a water miscible solvent, such as acetone or ethanol. The solution is then poured or injected into an aqueous solution containing stabilizer under magnetic stirring (Pal *et al.*, 2011). Nanoparticles are formed instantaneously by the rapid solvent diffusion (Pal *et al.*, 2011). The solvent is then removed from the suspensions under reduced pressure (Pal *et al.*, 2011).

1.5.6. Ionic gelation method or coacervation

Polymers with the property of biodegradability is highly being used recently, such as gelatin and sodium alginate as they offer properties like biocompatibility and low toxicity, which is quite safe in the therapeutic uses (El-shabouri *et al.*, 2002). Ionic gelation process can be used for preparing hydrophilic polymer based nanoparticles. This method was developed for preparing chitosan based nanoparticles by ionic gelation method or coacervation method (El-shabouri *et al.*, 2002). In coacervation method two different aqueous phases are prepared for polymer, like chitosan, and the other is for polyanion sodium tripolyphosphate. This process is based on the strong electrostatic interaction between the amino group of chitosan, which is positively charged and tripolyphosphate, which is negatively charged to form nanosized coacervates (El-shabouri *et al.*, 2002). Presence of strong electrostatic interaction between two aqueous phases leads to the formation of coacervates. Also it can be said that, ionic gelation involves the material undergoing transition from liquid to gel due to ionic interaction conditions at room temperature (El-shabouri *et al.*, 2002).

1.6. Characterization of nanoparticles

Characterization of nanoparticles is done employing following methods.

1.6.1. Structural evaluation

In the field of pharmacy, structure can be the difference between life and death, slight alteration or a big change in structural configuration may lead to adverse effects even death (Chidambaram & Krishnasamy, 2014). This makes necessary to confirm the purity of drug and excipients as well as their compatibility to produce positive effects on the subject (Chidambaram & Krishnasamy, 2014).

1.6.1.1. Fourier transform infrared spectroscopy (FTIR)

This method helps to study the functional groups present in the sample. Each functional group possesses one or more characteristic peaks at different wave numbers (Chen *et al.*, 2015). This qualitative analysis evaluates any interaction between drug and excipients or any change of functional group during the formulation (Chen *et al.*, 2015).

1.6.1.2. Nuclear magnetic resonance (NMR)

Since most of the drugs are organic molecules, NMR can be employed for the purity assessment of the samples as well as the drug-excipient compatibility studies. Generally ^1H NMR is used in the preformulation studies of nanoparticles (Uğurbil *et al.*, 2018).

1.6.2. Thermal analysis

Differential scanning calorimetry (DSC) is a thermal analysis technique which measures the temperature and heat flow associated with transitions in materials as a function of temperature and time (Chiu *et al.*, 2011). Such thermal analysis measurements are useful to obtain qualitative and quantitative data about the physical and chemical changes, including changes in heat capacity, exothermic, and endothermic processes (Chiu *et al.*, 2011).

1.6.3. Crystallinity

For the evaluation of crystallinity and purity, X-ray diffraction (XRD) method is used (Bunaciu *et al.*, 2015). The principle of XRD is based on Bragg's equation, which depends on the angle of incidence on crystal surface and distance between atomic layers in a crystal (Bunaciu *et al.*, 2015). Bragg's equation is expressed as: $n \lambda = 2d \sin\theta$, where n is an integer, which stands for the order of reflection, λ is wavelength of the incident X-rays, d is the interplanar spacing of the crystal and θ is the angle of incident X-rays (Bunaciu *et al.*, 2015).

When X-rays pass on a crystal they are scattered based on the arrangement of atoms in the crystal (Bunaciu *et al.*, 2015). If there is any interaction between drug and excipients or loss of crystallinity takes place, it can be easily depicted by the nature of peaks (Bunaciu *et al.*, 2015).

1.6.4. Particle size

Particle size distribution and morphology are the most important parameters in the characterization of nanoparticles (Nahar *et al.*, 2006). Drug release and drug targeting are considered to be the critical factors for nanoparticles. It has been found that particle size affects the drug release and diffusion (Nahar *et al.*, 2006). There are several tools for determining the size of nanoparticles as discussed hereunder (Nahar *et al.*, 2006).

1.6.4.1. Dynamic light scattering (DLS)

Dynamic light scattering is widely used to determine the size of Brownian nanoparticles of nano to submicron range in colloidal suspensions (DeAssis *et al.*, 2008). Shining monochromatic light (laser) into a suspension of spherical particles in Brownian motion causes a Doppler shift when the light hits the moving particle, changing the wavelength of the incoming light (DeAssis *et al.*, 2008). This change is related to the size of the particle. Besides determination of size, polydispersity index can also be measured by this process (DeAssis *et al.*, 2008).

1.6.4.2. Transmission electron microscopy (TEM)

TEM is a microscopic technique in which a beam of electrons is transmitted through a specimen to form an image (Molpeceres *et al.*, 2000). The sample preparation for TEM is complex and time consuming because it required ultrathin object for the electron transmittance (Molpeceres *et al.*, 2000). The nanoparticles dispersion is deposited onto support grids or films (Molpeceres *et al.*, 2000). In this process, the nanoparticles are fixed using either a negative staining material, such as phosphotungstic acid or derivatives, uranyl acetate, etc, or by plastic embedding. Alternate method is to expose the sample to liquid nitrogen after embedding in vitreous ice. The surface characteristics of the sample are obtained when a beam of electrons is transmitted through an ultrathin sample, interacting with the sample as it passes through (Molpeceres *et al.*, 2000).

1.6.4.3. Atomic force microscopy (AFM)

This offers ultra-high resolution in particle size measurement and it is based on a physical scanning of samples at sub-micron level using a probe tip of atomic scale (Polakovic *et al.*, 1999). Instrument provides a topographical map of sample based on forces between the tip and the sample surface (Polakovic *et al.*, 1999). AFM provides the most accurate description of size and size distribution and requires no mathematical calculation (Polakovic *et al.*, 1999). Moreover, particle size obtained by AFM technique provides real picture, which helps in understanding the effects under various biological conditions (Polakovic *et al.*, 1999).

1.6.5. Surface charge

The nature and intensity of the surface charge of nanoparticles is very important as it determines their interactions with the biological environment as well as their electrostatic interactions with bioactive compounds (Pangi *et al.*, 2003). The colloidal stability is analyzed through zeta potential of nanoparticles (Pangi *et al.*, 2003). The extent of surface hydrophobicity can then be predicted from the values of zeta potential (Pangi *et al.*, 2003). The zeta potential can also provide information regarding the nature of material encapsulated within the nanocapsules or coated onto the surface (Pangi *et al.*, 2003).

1.6.6. Drug release

The *in vitro* drug release is quantified employing UV-visible spectroscopy or high performance liquid chromatography (HPLC) (Magenhein *et al.*, 1993). Drug release

assays are also similar to drug loading assay, which is assessed for a period of time to analyze the mechanism of drug release (Magenhein *et al.*, 1993).

1.7. Objective of study

Carnosic acid (CA) has been found to be poorly water soluble and is only 40% bioavailable in rats (Doolaege *et al.*, 2011). Therefore, it has been aimed to improve the bioavailability of CA via formulating of CA-loaded PLGA nanoparticles. PLGA have been described as an effective nanocarrier for entrapping of various anti-cancer agents (Makadia *et al.*, 2011; Sithole *et al.*, 2018). The present research deals with formulation and characterization of CA-PLGA polymeric nanoparticles to intensify the bioavailability of CA.

Chapter 2

Literature review

Contents

- 2. Literature review
- 2.1. Literature review of CA
- 2.2. Literature review of PLGA
- 2.3. Literature review of TPGS
- 2.4. Literature review on success of nanoparticle formulation
- 2.5. Literature review on nanoprecipitation method

2. Literature review

The in-depth literature survey is required before executing any research work. Review of literature includes gathering all the appropriate information related to the research materials and research methodologies. Over past few decades, world wide web (Web) can give the up-to-date information of all the appropriate literature within a brief span of time. This chapter depicts all the relevant information of test materials to justify their crucial roles in the preparation of nanoparticles.

2.1. Literature review of CA

CA (Figure 2.1.) is a natural bezenediol diterpenoid with an abieta-8,11,13-triene substituted by hydroxy groups at positions 11 and 12 and a carboxy group at position 20 (Schwarz *et al.*, 1992). CA was first extrated by Linde and co-workers from *Salvia officinalis* (Figure 2.2.a) (family: Lamiaceae) (Linde *et al.*, 1964). However, CA was found in much higher levels (3% on weight basis in air-dried leaves) in leaves of *Rosmarinus officinalis* (Figure 2.2.b) (family: Lamiaceae) (Wenkert *et al.*, 1965). Dried leaves of rosemary or sage contain 1.5 to 2.5 % of CA (Karin *et al.*, 1992). CA is also found in trace quantity in *Origanum vulgare* (Figure 2.2.c) (family: Lamiaceae) (Hernández *et al.*, 2009). CA is not evenly distributed in all parts of the plants; however, it is mostly present in the aerial parts, mainly found in photosynthetic tissues, such as leaves, sepals, and petals (Karin *et al.*, 1992; Hernández *et al.*, 2009).

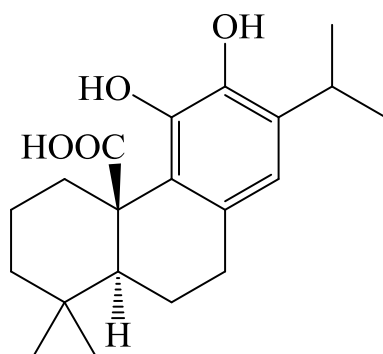


Figure 2.1. Structure of CA.



Figure 2.2. Major sources of CA, the leaves of *Salvia officinalis* (a), *Rosmarinus officinalis* (b), and *Origanum vulgare* (c).

2.1.1. Physico-chemical characteristics

Structural formula: $C_{20}H_{28}O_4$ (Schwarz *et al.*, 1992).

Molecular weight: 332.42 (Schwarz *et al.*, 1992).

IUPAC name: (4aR,10aS)-5,6-dihydroxy-1,1-dimethyl-7-propan-2-yl-2,3,4,9,10,10a-hexahydrophenanthrene-4a-carboxylic acid (Das *et al.*, 2018)

Solubility: CA is found to be lipophilic in nature (Xie *et al.*, 2017). It is soluble in organic solvents like, acetone, ethyl acetate, dimethylformamide, DMSO, ethanol and sparingly soluble in aqueous buffer (Birtic' *et al.*, 2015).

2.1.2. Therapeutic properties

Over the last decade, several research teams studied the pharmacological properties of CA (Birtic' *et al.*, 2015). Research over the past decade indicates that CA has multiple bioactive properties (Figure 2.3.) including antioxidant (Morán *et al.*, 2012), anti-inflammatory (Reuter *et al.*, 2007) and anticancer activities (Baliga *et al.*, 2013). Besides it is useful in cardiac injuries, atherosclerosis, brain injuries, Parkinson's disease, retinal degeneration, obesity, skin lesions and gastric lesions (Das *et al.*, 2018).

2.1.2.1. Anticancer property

CA-enriched extract was found to possess anti-cancer activity due to its pro-apoptotic, antiproliferative, chemoprotective, antitumour, and antiplatelet properties (Nabekura *et al.*, 2010; Baliga *et al.*, 2013). Treatment with CA at 1 and 10 mM for 48 h has been found to attenuate the proliferation of HT-29 colon adenocarcinoma cells (Kim *et al.*, 2014). It has been reported that CA possesses antiproliferative action on a group of human colon cancer cell lines (Borrás-Linares *et al.*, 2015). It was also

reported that CA can trigger autophagic cell death in human hepatoma cells (Gao *et al.*, 2015).

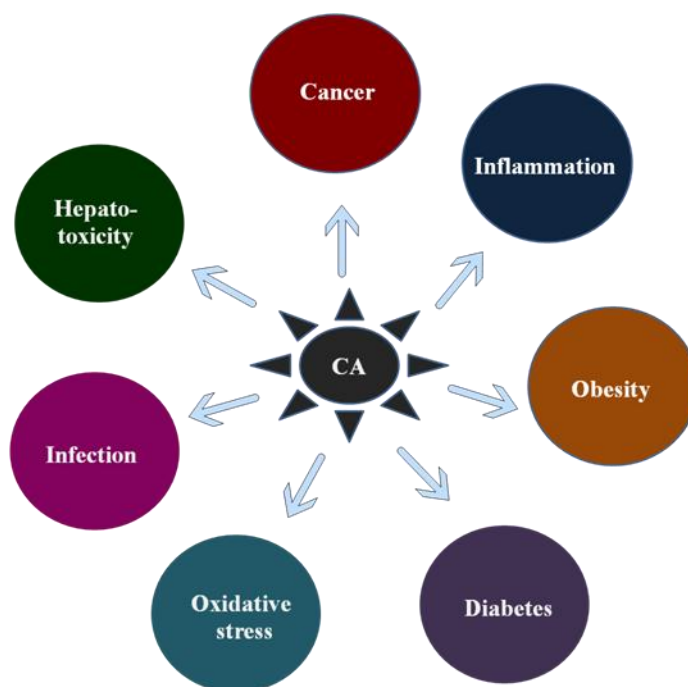


Figure 2.3. CA cures several complications.

2.1.2.2. Antiobesity property

CA has been reported to possess anti-adipogenic properties enabling weight loss i.e. antiobesity activity (Gaya *et al.*, 2013). CA exhibited body-weight, energy metabolism, and inflammation regulatory properties (Gaya *et al.*, 2013). CA has been found to cause selective modulation of caecum microbiota, inhibition of β -glucosidase activity, modulation of fecal excretion of fiber and short chain fatty acids in obese female rats (Harach *et al.*, 2010).

2.1.2.3. Antidiabetic property

It has been proven that CA is efficiently alleviate hyperglycaemia (Dickmann *et al.*, 2012). CA has been found to possess an insulin-like effect. It promotes glucose uptake by glycogenesis and inhibits gluconeogenesis by the hepatocytes (Shan *et al.*, 2015).

2.1.2.4. Antiinflammatory property

CA has been shown to exhibit anti-inflammatory activity (Reuter *et al.*, 2007). The anti-inflammatory effect was revealed by the reduction of circulating interleukins,

leptin, adiponectin and tumor necrosis factor- α levels in rats (Romo-Vaquero *et al.*, 2014).

2.1.2.5. Antimicrobial property

Rosemary extracts enriched with CA have been shown to have antimicrobial activity against various pathogens (Moreno *et al.*, 2006).

2.1.2.6. Antioxidant property

CA is principally known for its antioxidant and radical scavenging effects (Das *et al.*, 2018). It has been found to attenuate xenobiotic-provoked oxidative stress (Das *et al.*, 2018). Oral health care is another cosmetics-related application of CA (Morán *et al.*, 2012).

2.1.2.7. Hepatoprotective property

CA has been reported to exhibit preventive action on palmitate-induced lipid accumulation in hepatocytes indicating that CA may potentially block cellular lipid accumulation in the long term use (Park and Mun, 2013).

2.1.3. Uses

CA has a significant role in the food and cosmetics industries as food additives or nutraceutical or cosmeceutical (Birtic' *et al.*, 2015). CA (5-20 %) has been regarded as food additives by the European Union (Birtic' *et al.*, 2015; Aguilar *et al.*, 2008). Due to its high antioxidant activity, it can enhance the shelf life of the food products, such as vegetable and fish oil, meat, and patties via protection from oxidative damage (Birtic' *et al.*, 2015). In most cases, CA has been chosen over synthetic antioxidants as a natural preservative (Birtic' *et al.*, 2015; Aguilar *et al.*, 2008).

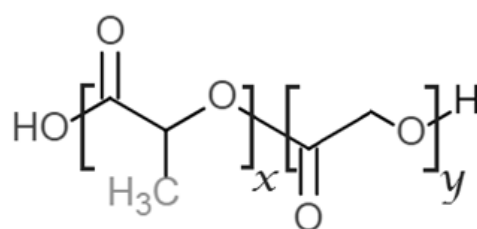
2.1.4. Low bioavailability and hydrophobic nature of CA

It has been reported that CA is hydrophobic in nature (Xie *et al.*, 2017). Hydrophobicity leads to poor bioavailability (Schrapp and Opperhuizen, 1990). Low bioavailability of CA has been mentioned in different investigations (Yan *et al.*, 2009; Doolaege *et al.*, 2011). It has been reported that 6 h after oral administration in rats (64.3 ± 5.8 mg/kg), the bioavailability of CA in its free form was found to be 40.1 % (Doolaege *et al.*, 2011).

2.2. Literature review of PLGA

Depending on the ratio of lactide to glycolide used for polymerization, different forms of PLGA polymers can be obtained: these are usually identified in regard to molar ratio of the monomers used, e.g. PLGA 75:25 means a copolymer composing 75% of

lactic acid and 25% of glycolic acid, whose molecular weight is ranging between 66000 and 107000 (Makadia *et al.*, 2011). PLGA has attracted considerable attention due to its attractive properties, like biodegradability and biocompatibility (Hans *et al.*, 2002). US-Food and Drug Administration and European Medicine Agency approved PLGA in drug delivery systems for parenteral administration (Hans *et al.*, 2002). It is applicable for diverse types of molecules, such as lipophilic, lipophobic, micromolecules, and macromolecules (Hans *et al.*, 2002). In addition, PLGA has been found to protect drug from degradation, to ensure sustained release of drug, to modify surface properties, and to target nanoparticles to the specific organs or cells (Hans *et al.*, 2002).



x= number of lactic acid monomer

y= number of glycolic acid monomer

Figure 2.4. Structure of PLGA.

2.2.1. Applications of PLGA-based nanoparticles

PLGA-based nanotechnology has been developed for several years and has been approved by the US-Food and Drug Administration for the use of drug delivery, diagnostics, and other applications in clinical and basic science research, including cardiovascular disease, cancer, vaccine, and tissue engineering (Lü *et al.*, 2009). It has been widely used to formulate into different biodegradable devices, such as microparticles, nanoparticles, implants and miscellaneous devices (Danhier *et al.*, 2012).

2.2.2. Physico-chemical properties of PLGA

Unlike pure polylactic and pure polyglycolic acid, PLGA can be dissolved by a wide range of common solvents, including chlorinated solvents, tetrahydrofuran, acetone or ethyl acetate (Zhu *et al.*, 2000). It can be processed into any shape and size, and can encapsulate biomolecules of any size. Physical properties of PLGA depend on different factors, such as the initial molecular weight of the monomers, the lactic

acid:glycolic acid ratio, and the exposure time to water and the storage temperature (Kumar *et al.*, 2006).

As two enantiomeric isomers of lactide exist (e.g., D and L, according to the position of pendant methyl group on the α carbon of poly lactic acid), PLGA is available as D-, L-, and D,L-isomers. Although glycolic acid lacks the methyl side group (in contrast to lactic acid), making it highly crystalline, and PLGA copolymers are amorphous (Gentile *et al.*, 2014).

PLGA degrades by hydrolysis of its ester linkages, through bulk or heterogeneous erosion, in aqueous environments as following steps (Makadia *et al.*, *et al* 2011). Water penetrates into the amorphous region and disrupts the van der Waals forces and hydrogen bonds, causing a decrease in the glass transition temperature (T_g); cleavage of covalent bonds takes place, with a decrease in the molecular weight; carboxylic end group autocatalyzes the degradation process, and mass loss begins by massive cleavage of the backbone covalent bonds resulting in loss of integrity; the fragments are further cleaved to molecules that are soluble in the aqueous environment (Makadia *et al.*, *et al* 2011). After the degradation, lactic acid and glycolic acid are formed as by-products (Kumar *et al.*, 2007).

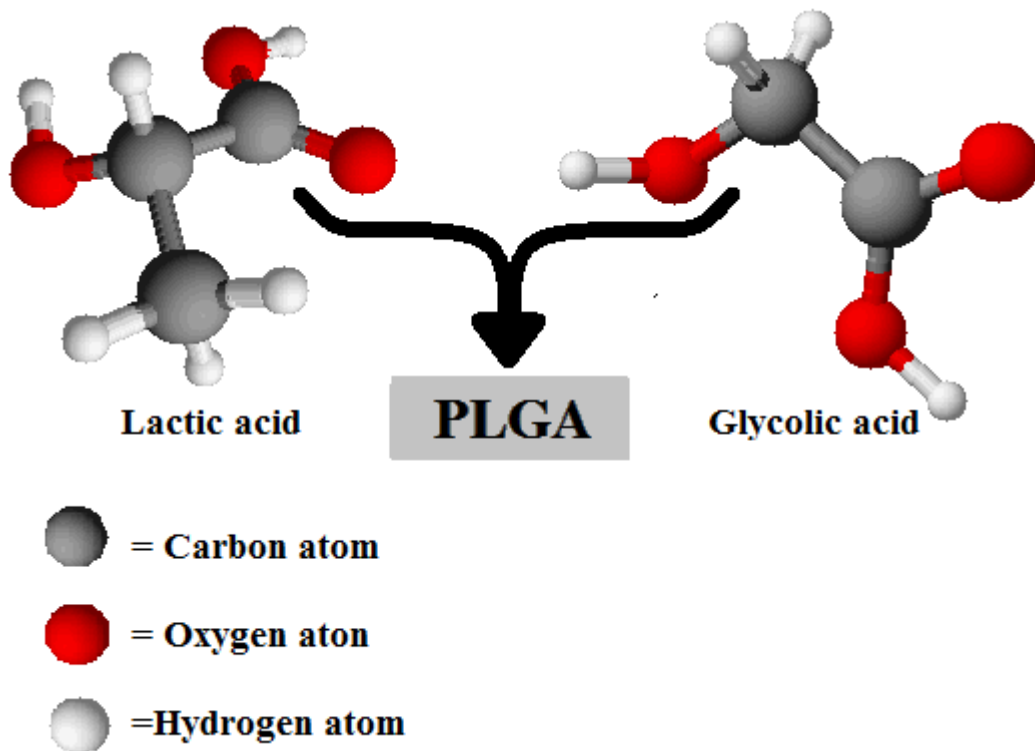


Figure 2.5. Formation of PLGA from lactic acid and glycolic acid monomer.

2.2.3. Drug release behavior

PLGA copolymer undergoes degradation by hydrolysis or biodegradation through cleavage of its backbone ester linkages into oligomers and, finally monomers. The degradation process for these polymers is mainly through uniform bulk degradation of the matrix, where the water penetration into the matrix is higher than the rate of polymer degradation (Joshi *et al.*, 2011). Furthermore, the increases in the carboxylic groups as a result of biodegradation can autocatalyse the process of degradation (Joshi *et al.*, 2011). The degradation of PLGA copolymer is the collective process of bulk diffusion, surface diffusion, bulk erosion, and surface erosion. There are many variables, which influence the degradation process. However, the release rate is often unpredictable (Hamdy *et al.*, 2011). The biodegradation rate of the PLGA copolymers is dependent on the molar ratio of the lactic and glycolic acids in the polymer chain, molecular weight of the polymer, the degree of crystallinity, and the Tg of the polymer. The release of drug from the homogeneously degrading matrix is more complicated (Gazi and Martinez-Pomares Martinez-Pomares, 2009). The PLGA polymer is biodegraded into lactic and glycolic acids. Lactic acid enters the tricarboxylic acid cycle and is metabolized and subsequently eliminated from the body as carbon dioxide and water (Cruz *et al.*, 2010). Glycolic acid is either excreted unchanged in the kidney or it enters the tricarboxylic acid cycle and is also eliminated as carbon dioxide and water (Cruz *et al.*, 2010).

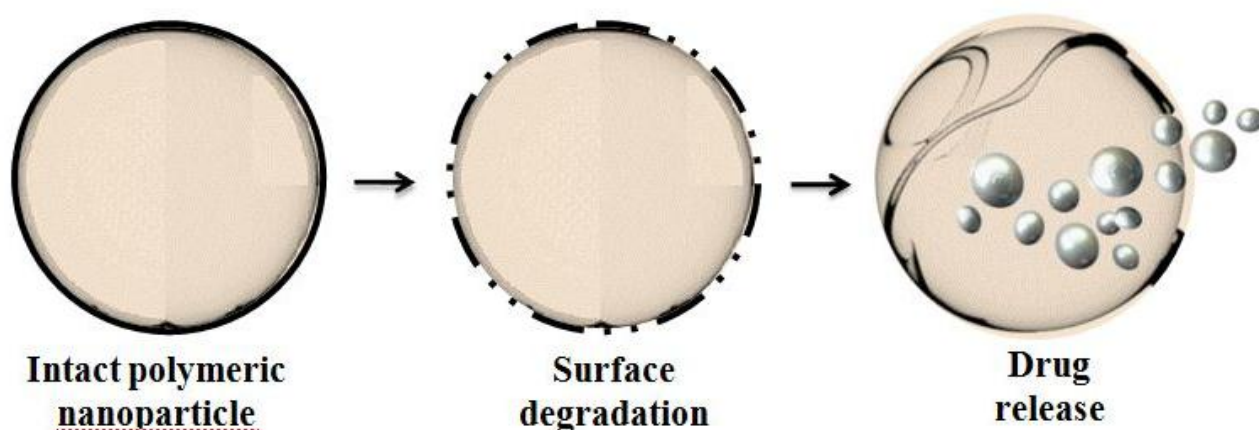


Figure 2.6. Drug release from PLGA nanoparticles.

2.2.4. Factors affecting degradation of PLGA

To enhance the desirable properties of PLGA, it is essential to understand the factors affecting the PLGA degradation and design a drug delivery device accommodating all these factors to make it more efficient and efficacious.

2.2.4.1. Effect of composition

Polymer composition is the most important factor to determine the hydrophilicity and rate of degradation of a delivery matrix which influence the rate of degradation. A systematic study of polymer composition with its degradation has been shown by many groups (Von and Bochner, 2008; Jandus *et al.*, 2011). The results showed that increase in glycolic acid percentage in the oligomers accelerates the weight loss of polymer. PLGA 50:50 exhibited a faster degradation than PLGA 65:35 due to preferential degradation of glycolic acid proportion assigned by higher hydrophilicity. Subsequently, PLGA 65:35 shows faster degradation over PLGA 75:25 and PLGA 75:25 degrade faster than PLGA 85:15 (Scott *et al.*, 2008). Thus absolute value of the degradation rate increases with the glycolic acid proportion. Therefore, the amount of glycolic acid is a critical parameter in tuning the hydrophilicity of the matrix, degradation, and drug release rate (Scott *et al.*, 2008).

2.2.4.2. Effect of crystallinity

Copolymer composition also affects important properties such as glass transition temperature and crystallinity, which have indirect effects on degradation rate (Rajapaksa *et al.*, 2010).

2.2.4.3. Effect of weight average molecular weight (M_w)

Polymers with higher molecular weight have generally exhibited lower degradation rates. Molecular weight is directly proportional to the polymer chain size. Polymers with higher molecular weight require more time to degrade than small polymers (Garinot *et al.*, 2007).

2.2.4.4. Effect of drug types

The mechanism of polymer-drug matrix degradation and the parameters involved in drug release rate vary as a function of drug types (Fernandez *et al.*, 2012). The presence of drug may change the degradation mechanism from bulk erosion to surface degradation. It also affects the rate of matrix degradation (Vasir and Labhsetwar, 2008). The drug release profile, as defined by the time required to release 100 % of drug and the steady-state rate also varies significantly. However, efforts to correlate

the release rate parameters to the drug chemistry, such as the density of OH groups or hydrophilicity do not yield a strong relationship (Vasir and Labhasetwar, 2008).

2.2.4.5. Effect of size and shape of the matrix

The ratio of surface area to volume has shown to be a significant factor for degradation of large devices (Rajapaksa *et al.*, 2010). Higher surface area ratio leads to higher degradation of the matrix (Zhang *et al.*, 2011). It has also been reported that bulk degradation of PLGA is faster than pure surface degradation, which makes the release of the drug faster from the devices with higher surface area to volume (Hanlon *et al.*, 2011).

2.2.4.6. Effect of pH

Both alkaline and strongly acidic media accelerate polymer degradation (Yaguchi *et al.*, 2011). However, the difference between the slightly acidic and neutral media is less pronounced due to autocatalysis by the carboxylic end groups (Molavi *et al.*, 2010).

2.2.4.7. Effect of drug load

Amount of drug loading in the drug delivery matrix plays a significant role in the rate and duration of drug release. Matrices having higher drug content possess a larger initial burst release than those having lower content because of their smaller polymer to drug ratio (Roy *et al.*, 2010).

2.2.5. Role of PLGA as carrier of hydrophobic drugs

Drugs having low bioavailability require to be administered at higher dose; but it may cause toxicity (Thakkar *et al.*, 2010; Ezzat *et al.*, 2019). Water insoluble drugs often possess greater affinity for hydrophobic solvents because of hydrophobic-hydrophobic interactions and also have affinity for hydrophobic region of polymeric micelles (Thakkar *et al.*, 2010; Ezzat *et al.*, 2019). Hence encapsulation of those drugs in micelles enables their formulation in aqueous vehicle (Kalepu and Nekkanti, 2015). By encapsulation of the hydrophobic drugs, these can be protected from early metabolism as well as targeted drug delivery can also be achieved (Sithole *et al.*, 2018). PLGA nanoparticles are described in the literature as effective nanocarriers for the encapsulation of various anti-cancer agents (Makadia *et al.*, 2011). It has been reported that PLGA is used for encapsulation of hydrophobic drugs. PLGA nanoparticles loaded with hydrophobic and poorly soluble drugs are most commonly formulated by nanoprecipitation (Kumari *et al.*, 2010). Nanoprecipitation technique is

also known as solvent displacement method. In this method, two different phases are separately prepared. First one is organic phase and second one is aqueous phase. Organic phase consists of drug and polymer, which should be dissolved in water miscible solvents like methanol, acetone, DMSO etc. and aqueous phase consists of water soluble stabilizer (Gaonkar *et al.*, 2017).

2.3. Literature review of TPGS

It is also known as vitamin E TPGS. It is formed by the esterification of vitamin E succinate with polyethylene glycol 1000 (Wei *et al.*, 2014). As novel nonionic surfactant, it exhibits amphiphilic properties and can form stable micelles in aqueous vehicles at low concentration (Choudhury *et al.*, 2017). It is a water miscible form of vitamin E, is composed of a hydrophobic vitamin E part and a hydrophilic polyethylene glycol (PEG) chain. It exhibits excellent drug delivery capability based on this special amphiphilic structure (Choudhury *et al.*, 2017). The lipophilic alkyl tail is derived from tocopherol succinate while its hydrophilic polar head portion is formed from PEG making the surfactant structure bulky, hence with greater surface area (Wei *et al.*, 2014). The biological and physicochemical properties of TPGS provide multiple advantages for its applications in drug delivery like biocompatibility, enhanced drug solubility, improvement of the drug permeation and selective antitumor activity (Feng *et al.*, 2002).

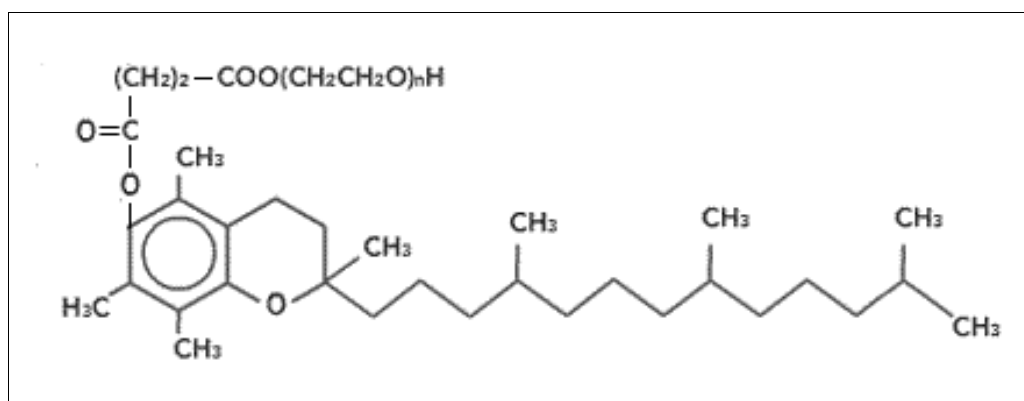


Figure 2.7. Structure of TPGS.

2.3.1. Physico-chemical characteristics

Chemical name: D- α -Tocopheryl polyethylene glycol succinate (Yang *et al.*, 2018).

Empirical Formula: $C_{33}O_5H_{54}(CH_2CH_2O)_n$ (Yang *et al.*, 2018)

Molecular Weight: Approximately 1513 (Yang *et al.*, 2018)

Physical form: Waxy solid (Yang *et al.*, 2018)

Melting point: 38°C (Yang *et al.*, 2018)

Solubility in water: Miscible in all parts (Yang *et al.*, 2018)

2.3.2. Suitability of TPGS with cancer drugs and PLGA nanoparticles

The chemical structure of the emulsifier TPGS is similar to other amphiphile molecule structures consisting of alkyl tail, which is lipophilic in nature and polar head portion, which is hydrophilic in nature (Wei *et al.*, 2014). Its massive structure and huge surface area make it an outstanding emulsifier, which leads to the miscibility of hydrophobic compounds in the aqueous media (Yang *et al.*, 2018). It has been found that administering TPGS along with anticancer drugs can trigger cytotoxicity, inhibit P-glycoprotein mediated multi-drug resistance, and increase oral bioavailability of anticancer drugs (Gaohua *et al.*, 2017). In addition, it has been reported that TPGS is suitable emulsifier for the preparation of PLGA nanoparticles (Gaonkar *et al.*, 2017). TPGS can induce apoptosis and exhibits selective cytotoxic effects against cancer cells, which can be combined with chemotherapeutic drugs to reduce side effects and to increase therapeutic efficiency. There was significant different response on normal immortalized breast cells and cancer cells after TPGS treatment (Neophytou *et al.*, 2014). TPGS can trigger the apoptotic signaling pathways and induce G1 and S cell cycle arrest in breast cancer cells (Neophytou *et al.*, 2014). Poor water solubility and/or poor permeability remain as the major obstacles for therapeutic drugs to exert maximum activity. TPGS can be applied as solubilizer, absorption, permeation enhancer, emulsifier, and surface stabilizer in drug delivery (Yang *et al.*, 2018). It has been widely used in fabricating purpose of many nanodrugs or other formulations for many poorly water-soluble or permeable drugs (Yang *et al.*, 2018). As a surfactant and emulsifier, TPGS shows outstanding capability to increase drug absorption through different biological barriers (Yang *et al.*, 2018).

2.4. Literature review on success of nanoparticle formulations

2.4.1. Comparison between pharmacokinetic model of vinpocetine solution and nanoparticle

On studying one-compartment model describing the GI tract and blood compartment and elimination from the blood compartment, it was found that Vinpocetine solution fits better in one-compartment model than two-compartment model, as vice versa

result was found in the case of Vinpocetine nanoparticles (Luo *et al.*, 2006). The nanoparticles enloaded with Vinpocetine results in 4.5 times lower apparent clearance, 1.7 times lower apparent volume of distribution, and 1.8 times longer apparent circulation half-life than the plain drug (Luo *et al.*, 2006).

2.4.2. Bioavailability improvement of apigenin by carbon nanopowder entrapment

In this study, carbon nanopowder was used as drug carrier intended to enhance oral bioavailability of Apigenin, an anticancer phytoconstituent having low bioavailability (Ding *et al.*, 2014). Solid dispersion of Apigenin was compared with Apigenin enloaded carbon nanopowder on the basis of pharmacokinetic aspect and *in vivo* performances (Ding *et al.*, 2014). The physicochemical properties of the formulations were examined by differential scanning calorimetry, X-ray diffraction, and scanning electron microscopy (Ding *et al.*, 2014). Drug release profile of Apigenin was reported to be improved by 275% compared with that of pure Apigenin. *In vivo* studies showed that bioavailability of pure Apigenin was significantly improved (Ding *et al.*, 2014). In another report it was shown that entrapment of Apigenin in polymeric nanoparticles achieves better results both in pharmacokinetic and pharmacodynamic aspect (Bhattacharya *et al.*, 2018).

2.4.3. Improvement pharmacokinetic and pharmacodynamical profile of clozapine by formulating solid lipid nanoparticles

Antipsychotic drug, Clozapine has very poor oral bioavailability (below 27%) due to first pass metabolism (Manjunath & Venkateswarlu, 2005). By hot homogenization Clozapine solid lipid nanoparticles have been developed using various triglycerides like trimyristin, tripalmitin and tristearin, soylecithin 95%, poloxamer 188 and stearylamine (Manjunath & Venkateswarlu, 2005). On the pharmacokinetic study of Clozapine incorporated in solid lipid nanoparticles on intravenous administration to conscious male Wistar rats and tissue distribution studies of Clozapine solid lipid nanoparticles and suspension on Swiss albino mice it was revealed that the therapeutic window was increased up to 2.91 times and clearance was decreased up to 2.93 times than that of Clozapine suspension and bioavailability of Clozapine solid lipid nanoparticles were 2.45 to 4.51 times higher than that of Clozapine suspension (Manjunath & Venkateswarlu, 2005).

2.4.4. Candesartan cilexetil nanoparticles incorporated tablet showed better therapeutic effect over conventional candesartan cilexetil tablets

Sparingly water-soluble drug Candesartan cilexetil is an angiotensin receptor blocker, used as antihypertensive agent, was incorporated in nanoparticles to increase its saturation solubility and dissolution rate for enhancing bioavailability while reducing variability in systemic exposure (Nekkanti *et al.*, 2009). This report showed that tablet formulation incorporating Candesartan cilexetil nanoparticles has significantly faster rate of drug dissolution in the dissolution medium as compared to commercially available tablet formulation (Nekkanti *et al.*, 2009). Systemic exposure studies in rats indicated a significant increase in the rate and extent of drug absorption (Nekkanti *et al.*, 2009)

2.4.5. Curcumin enloaded nanoparticles shows better antimicrobial activity over pure curcumin

Curcumin is a phytoconstituent, being used from the ancient time period, which is known to have antimicrobial property, but also has poor bioavailability (Pandit *et al.*, 2015). Curcumin enloaded nanoparticles showed high efficacy against bacteria, like *Escherichia coli*, *Staphylococcus aureus*, and *Pseudomonas aeruginosa* (Pandit *et al.*, 2015). It was reported that Curcumin enloaded nanoparticles incorporated in cream synthesized by sonication method inhibited activity of bacteria (Pandit *et al.*, 2015), which approach was better in comparison with conventional formulation. The formulated cream is new generation of antiseptic cream, which could be used in the treatment of infection caused by *Escherichia coli*, *Staphylococcus aureus*, and *Pseudomonas aeruginosa* (Pandit *et al.*, 2015).

2.5. Literature review on nanoprecipitation method

The nanoprecipitation method was reported as an easy and productive preparation method of nanoparticles (Pal *et al.*, 2011). This method basically requires preparation of two separated phases: organic and aqueous. In brief, the organic phase consists of polymer and the drug to be incorporated and the aqueous phase consists of emulsifier; which on interaction with each other produce polymeric nanoshells, followed by stirring, solvent evaporation and lyophilisation (Pal *et al.*, 2011).

Nanoprecipitation method was found to be applicable for both hydrophilic and hydrophobic drugs (Salatin *et al.*, 2017; Alshamsan *et al.*, 2013). Development of polymeric nanoparticles (Salatin *et al.*, 2017; Gaonkar *et al.*, 2017; Alshamsan *et al.*,

2013). For example, using nanoprecipitation method entrapment of a very water soluble drug into Eudragit nanoparticles was reported a successful approach. Co-administration of TPGS with PLGA polymers in nanoprecipitation technique yielded high amount of polymeric nanoparticle (Gaonkar *et al.*, 2017). Also high entrapment efficiency of hydrophilic drug substances in nanoparticles was achieved using nanoprecipitation (Peltonen *et al.*, 2009) Beside drug enloaded nanoparticle production, nanoprecipitation was also used for the production of protein-loaded PLGA nanospheres (Morales-Cruz *et al.*, 2012). Another report shows that nanoprecipitation technique is more efficient than emulsion solvent evaporation method (Alshamsan *et al.*, 2013).

Chapter 3

Materials and methods

Contents

3.1. Materials

3.2. Methods

3.2.1. Preparation of CA loaded nanoparticles

3.2.2. Determination of λ_{\max} of CA

3.2.3. Plotting standard curve of CA in ethyl acetate

3.2.4. Characterisation of nanoparticles

3.2.5. *In vitro* drug release study

3. Materials and methods

3.1. Materials

CA was purchased from TCI Chemicals (India) Pvt. Ltd. PLGA 75:25 (PURASORB PDLG 5010) was obtained as a gift from Purac Biomaterials. Vitamin E TPGS NF Grade was gifted by Antares Health Products. Acetone, Ethyl acetate and other chemicals were purchased from Merck Life Sciences Private Limited, India.

3.2. Methods

3.2.1. Preparation of CA loaded nanoparticles

Nanoparticles were prepared by the nanoprecipitation method (Pal *et al.*, 2011) (Figure 3.1.). In this method, one organic phase and one aqueous phase were prepared separately (Gaonkar *et al.*, 2017). The organic solution of PLGA and CA in varying ratios (Table 3.1.) were dissolved in acetone (10 ml) and mixed well, as CA is soluble in acetone (Birtic' *et al.*, 2015), this was used to prepare the organic phase. Simultaneously, the aqueous solution was prepared in a beaker by mixing the emulsifier vitamin E TPGS (0.03% w/v) in distilled water (20 ml) employing magnetic stirrer at moderate speed at room temperature until the emulsifier completely dissolves (Gaonkar *et al.*, 2017). As TPGS is water miscible compound, it dissolved within few minutes. Then the organic solution is poured into the aqueous solution without switching off the magnetic stirrer. As soon as two phases were mixed, the solution became turbid, which indicated the formation of polymeric shells (Gaonkar *et al.*, 2017). The solvent was allowed to evaporate overnight. Being volatile acetone evaporates and the solution becomes concentrated (Chien *et al.*, 2017). The suspension obtained was filtered with filter paper to remove any precipitate and then it was centrifuged at 18,000 rpm at 4°C temperature (Sorvall RC 5 Plus, US). The supernatant containing the free drug was discarded and the pellet obtained was washed 2-3 times with distilled water and lyophilized in lyophiliser (VirTis, US) for 48 h to get a free flowing powder. Placebo nanoparticles were prepared according to the same procedure. The prepared nanoparticle formulation was weighed and stored at 0 °C temperature. This method was performed in triplicate (n = 3).

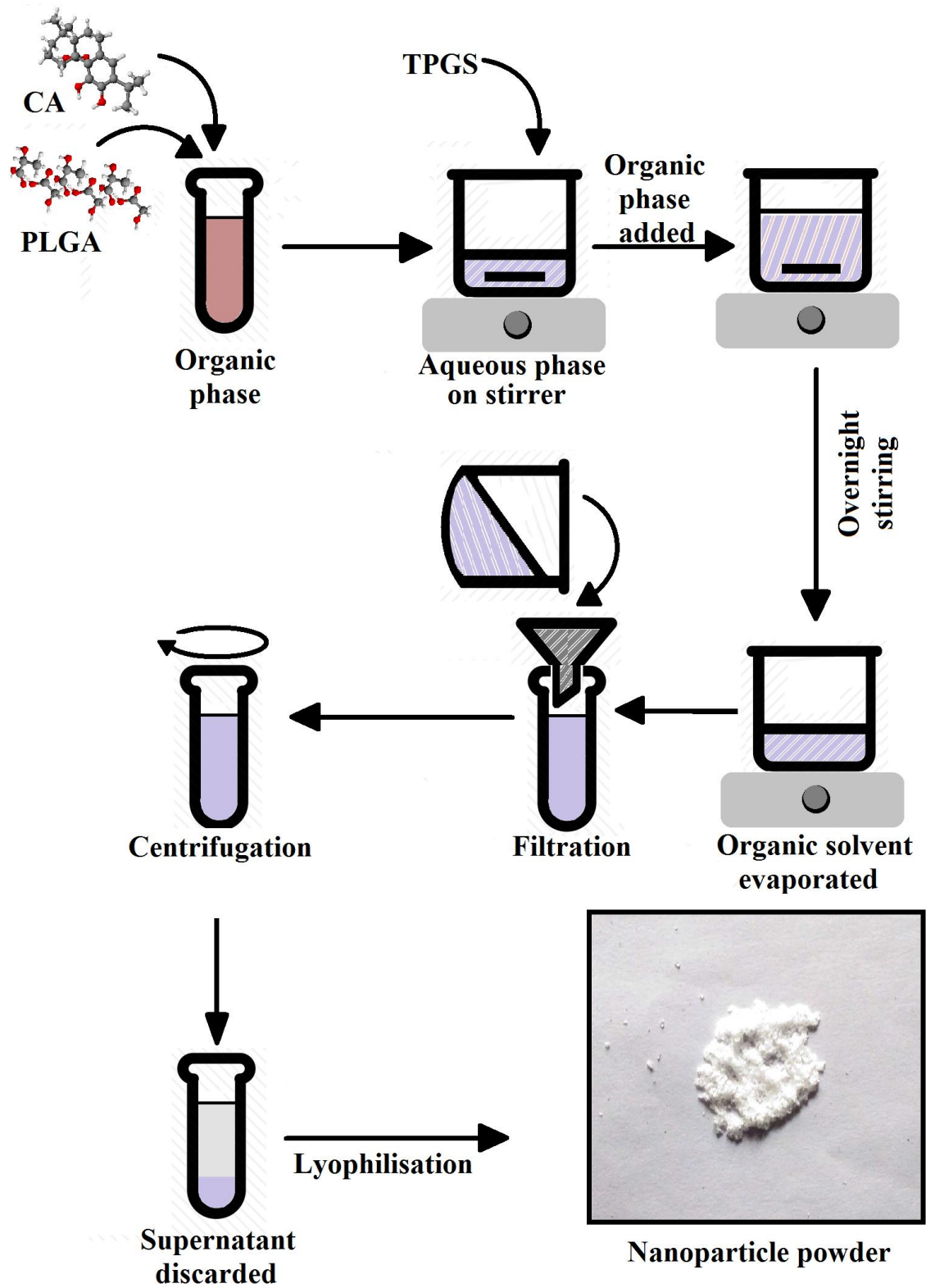


Figure 3.1. A schematic overview of CA nanoparticle preparation method.

Table 3.1. Amounts of drug and polymer used in nanoparticle formulation.

Drug : Polymer	Polymer fed initially (mg)	Drug fed initially (mg)
1 : 6.66	50	7.5
1 : 10	50	5
1 : 20	50	2.5

3.2.2. Determination of λ_{\max} of CA

Solubility 1.5 mg CA was dissolved in 5 ml of ethyl acetate by sonication (Sawant *et al.*, 2011). Ethyl acetate was used as solvent, as CA is reported to be soluble in Ethyl acetate (Birtic' *et al.*, 2015). The solution of CA (300 $\mu\text{g/ml}$) was used for determination of λ_{\max} in UV-Vis spectrophotometer (Model Intech-295, India), at the scanning range of 200-400 nm against blank (Sawant *et al.*, 2011).

3.2.3. Plotting standard curve of CA in ethyl acetate

CA was dissolved in ethyl acetate and stock solution of 1mg/ml was made. Taking aliquots from stock solution CA solutions of various concentrations, ranging between 10-100 $\mu\text{g/ml}$ were prepared, diluting by Ethyl acetate. The absorbance was measured at λ_{\max} of CA at different concentrations in UV-Vis single beam spectrophotometer (Model Intech-295, India) to generate a standard calibration curve (Sawant *et al.*, 2011). The absorbance of ethyl acetate was subtracted from each absorbance value. This method was performed in triplicate ($n = 3$).

3.2.4. Characterisation of nanoparticles

3.2.4.1. Evaluation of drug-excipient interaction

In the NMR study, 5 mg of each sample CA, PLGA, and CA-PLGA mixture was weighed properly and dissolved in 1 ml CDCl_3 (Chloroform D) with the help of sonication until the compounds were dissolved in the solvent. This solutions were scanned for ^1H NMR spectra in a NMR spectrophotometer (Bruker DRX 300 MHz spectrometer, US) (Gaohua *et al.*, 2005).

In the FTIR spectroscopic study, all samples, such as CA, PLGA, TPGS, the physical mixture of CA with the excipients, and the CA nanoparticles were powdered properly and scanned over a wavenumber range of 4000–400 cm^{-1} in an inert atmosphere in

FTIR spectrophotometer (Bruker Optik, Germany) to understand the possible chemical interactions occurring between the drug and the polymer matrix (Gaonkar *et al.*, 2017).

3.2.4.2. Thermal analysis by DSC

The physicochemical compatibility between CA and the polymer was evaluated using a differential scanning calorimeter (Mettler Toledo, US). Accurately weighed samples (3 mg) of CA, PLGA, physical mixture of CA-PLGA, and CA nanoparticles were sealed separately in a standard aluminium pan heated over a temperature range from 30-300 °C at a constantly increasing rate of 10.00 °C/min in an atmosphere of nitrogen gas at a flow rate of 40 ml/min (Gaonkar *et al.*, 2017).

3.2.4.3. Crystallinity evaluation by XRD

XRD patterns of pure CA, polymer, mixture of CA and PLGA, and CA nanoparticles were measured in an X-ray powder diffractometer (XRD-2000, Rigaku, Japan). The measurements were performed in the 5-60° 2θ using CuKα radiation (45 kV, 40 mA) as the X-ray source and the rate of scanning was 1° /min to understand the possible chemical interactions occurring between the drug and the polymer matrix (Gaonkar *et al.*, 2017).

3.2.4.4. Nanoparticle yield (NY), drug loading (DL) and encapsulation efficiency (EE)

The freeze-dried nanoparticle samples (5 mg) were dissolved in ethyl acetate (5 ml) with the help of vortex for 5min and then sonication for 15min. Then it was taken for spectrophotometric measurement, where the absorbance values were noted and absorbance of blank nanoparticle (nanoparticle without drug) was subtracted. From the absorbance values the drug amount of drug in nanoparticles was quantified. NY, DL and EE of the prepared nanoparticles were quantified by measuring the absorbance at λ_{\max} of CA using a UV-Vis single beam spectrophotometer (Model Intech-295, India) and calculated from following three equations (Gaonkar *et al.*, 2017). This method was performed in triplicate (n=3).

$$\text{NY (\%)} = (\text{Weight of nanoparticles/Weight of polymer \& drug fed initially}) \times 100$$

$$\text{DL (\%)} = (\text{Weight of the drug in nanoparticles/Weight of nanoparticles}) \times 100$$

$$\text{EE (\%)} = (\text{Weight of the drug in nanoparticles/Weight of drug fed initially}) \times 100$$

3.2.4.5. Particle size measurements

3.2.4.5.1. TEM

The structure of CA nanoparticles was determined by TEM (Jeol JEM 2100F; JEOL-France). 2 mg CA nanoparticle was dissolved in 2 ml MilliQ water (1 mg/ml). A drop (10 μ l) of CA nanoparticle suspension, which was further diluted to 1/10 was placed carefully on a 300 mesh carbon coated copper TEM grid. The excess solution on the grid was removed using a tissue paper and the samples were air-dried for 8 hs. The dried sample was then examined at 120 kV under a microscope (Gaonkar *et al.*, 2017).

3.2.4.5.2. AFM

The shape of CA nanoparticle was further characterized by AFM (5500 Agilent Technologies, Santa Clara, CA, USA). A drop (10 μ l) of CA nanoparticle suspension (1 mg/ml) was placed on a mica sheet. The drop was allowed to air dry for 5-10 min. The sample was further mounted on the microscope scanner. The shape was observed and imaged in ACAFM mode with frequency 166.6 kHz and scan speed 0.502 μ m/s (Gaonkar *et al.*, 2017).

3.2.4.5.3. DLS

Particle size distribution (mean diameter and polydispersity index) was determined using a Malvern Zetasizer Nano ZS (Malvern Instruments, United Kingdom). Briefly, 1 mg/ml of CA nanoparticle suspension was prepared in MilliQ water by sonication for 30 s. The above suspension (10 μ l) was diluted to 1 ml with MilliQ water and analysis was performed (Gaonkar *et al.*, 2017).

3.2.4.6. Surface Charge

1 mg/ml of CA nanoparticle suspension was prepared in MilliQ water by sonication for 5min. The above suspension (10 μ l) was diluted to 1 ml with MilliQ water. This sample was used for the measurement of zeta potential at 25°C temperature using Malvern Zetasizer Nano ZS (Malvern Instruments, Worcestershire, United Kingdom) (Gaonkar *et al.*, 2017).

3.2.5. In vitro drug release study

3.2.5.1. Preparation of phosphate buffered saline (PBS)

Initially 50 ml PBS was prepared by mixing 3.87 ml of 1M Disodium hydrogen phosphate (Na_2HPO_4) and 1.13 ml of 1 M Sodium dihydrogen phosphate (NaH_2PO_4) and adjusting the volume upto 50 ml with distilled water. The pH was adjusted to 7.4

using Sodium hydroxide and Phosphoric acid (Gómez *et al.*, 2001) and was checked in pH meter. The pH of PBS was maintained at 7.4 as it matches the osmolarity and ion concentrations of the solution of the human body, (Gómez *et al.*, 2001) and we intended to prepare nanoparticle with better bioavailability.

3.2.5.2. Plotting standard curve of CA in PBS

The CA was dissolved in PBS buffer and stock solution of 1mg/ml was made. Taking aliquots from stock solution CA solutions of various concentrations, ranging between 5-50 $\mu\text{g/ml}$ were prepared, diluting by PBS. The absorbance was measured at λ_{max} of CA at different concentrations in UV-Vis single beam spectrophotometer (Model Intech-295, India) to generate a standard calibration curve (Sawant *et al.*, 2011). The absorbance of PBS was subtracted from each absorbance value. This method was performed in triplicate ($n = 3$).

3.2.5.3. Determination of cumulative percentage drug release

To determine the *in vitro* release of CA at various time intervals, CA nanoparticles (2 mg) were weighed accurately and they were suspended in 2 ml of PBS (pH 7.4). The suspension was sonicated for 5 min and subjected to vortex for 15 min. Then it was kept in incubator shaker at 37°C and the time counting was started. At preselected time intervals, 1 ml of the release media was taken out with micropipette and centrifuged (Spinwin, India) at 16000 rpm for 10 min; the supernatant (1ml) was collected for analysis. This supernatant contains the released drug which was subjected to UV-Vis single beam spectrophotometer (Model Intech-295, India). The absorbance of samples was noted each time. The absorbance of PBS was subtracted from each absorbance value. To the pellet containing nanoparticles with unreleased CA, an equal volume (1 ml) of fresh release media (PBS) was added. The mixture was transferred to original lot and the process continued. (Shaw *et al.*, 2017; Ozdal *et al.*, 2019). The unknown concentrations of the supernatants were determined plotting the respective values of absorbance in the standard curve of CA in PBS. After determining concentrations the amount of drug in each supernatant sample was calculated. The amount of drug released in each time interval was used for calculation of cumulative release percentage of CA from CA nanoparticles (Shaw *et al.*, 2017). This method was performed in triplicate ($n = 3$).

Chapter 4

Results and Discussion

Contents

- 4.1. λ_{\max} of CA
- 4.2. Standard curve of CA in ethyl acetate
- 4.3. $^1\text{H-NMR}$
- 4.4. FTIR
- 4.5. Thermal analysis by DSC
- 4.6. Crystallinity evaluation by XRD
- 4.7. NY, DL and EE
- 4.8. TEM
- 4.9. AFM
- 4.10. DLS
- 4.11. Surface Charge
- 4.12. Standard curve of CA in PBS
- 4.13. *In vitro* drug release study

4. Results and discussion

4.1. λ_{\max} of CA

λ_{\max} is the highest absorbance value in the graph of absorbance (x axis) versus wavelength (y axis) curve; the lowest possible concentration of a compound can be detected as it is the most accurate place to measure because of small errors in setting the wavelength in the spectrophotometer (Dastidar & Sa, 2009). The λ_{\max} value of CA was found to be 279 nm (Figure 4.1.) as measured in UV-Vis spectrophotometer (Model Intech- 295). It was reported in journal that λ_{\max} value of CA was 280nm (Luis & Johnson, 2005). So, it can be said, that the CA acid used in the project work was pure and the absorbance of CA solutions in different solvents should be measured at 279nm to get absorbance values with minimum error.

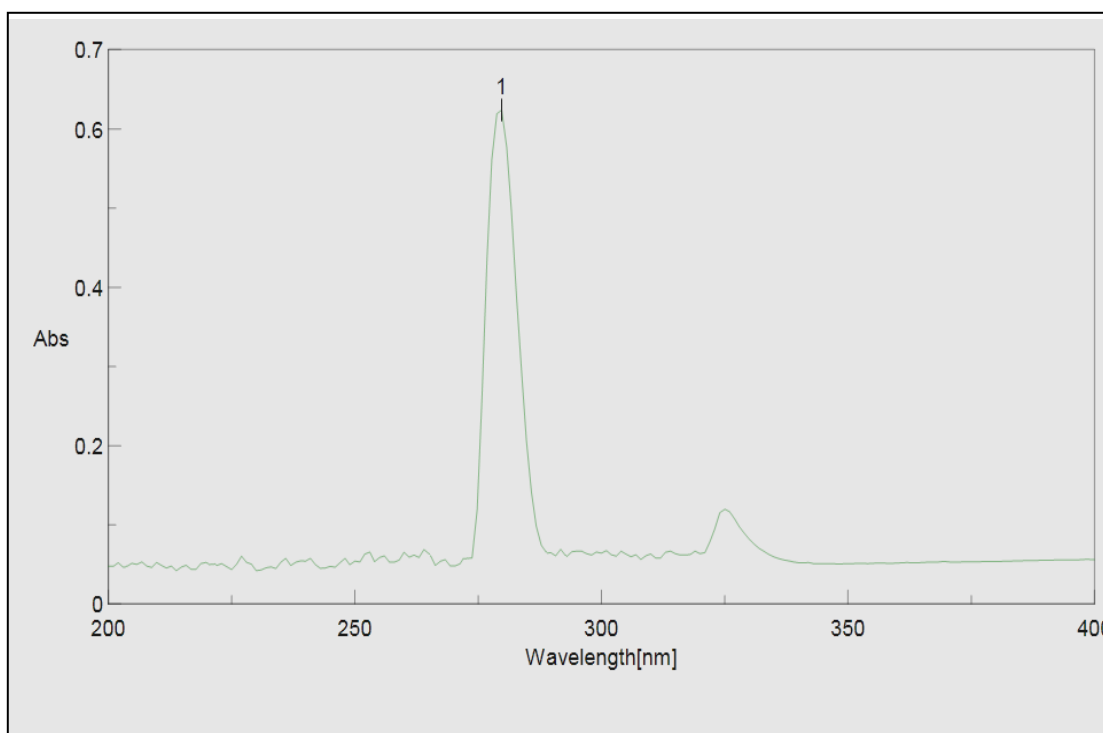


Figure 4.1. λ_{\max} of CA.

4.2. Standard curve of CA in ethyl acetate

Standard curve is based on the principle of Beer-Lambert's law, which states that, the quantity of light absorbed by a substance dissolved in a fully transmitting solvent is directly proportional to the concentration of the substance and the path length of the light through the solution (Baker et al., 2014) Plotting standard curve of a compound dissolved in a certain solvent helps in the determination of unknown concentration of

the solution of that compound (Dastidar & Sa, 2009). The standard curve of CA in ethyl acetate follows linearity (Figure 4.2.) and bears equation: $y = 0.0028x - 0.003$ (where x =concentration and y = absorbance) and have R^2 value 0.997. This equation shows that the increase in concentration of Ethyl acetate solution of CA is directly proportional to the increase of absorbance values.

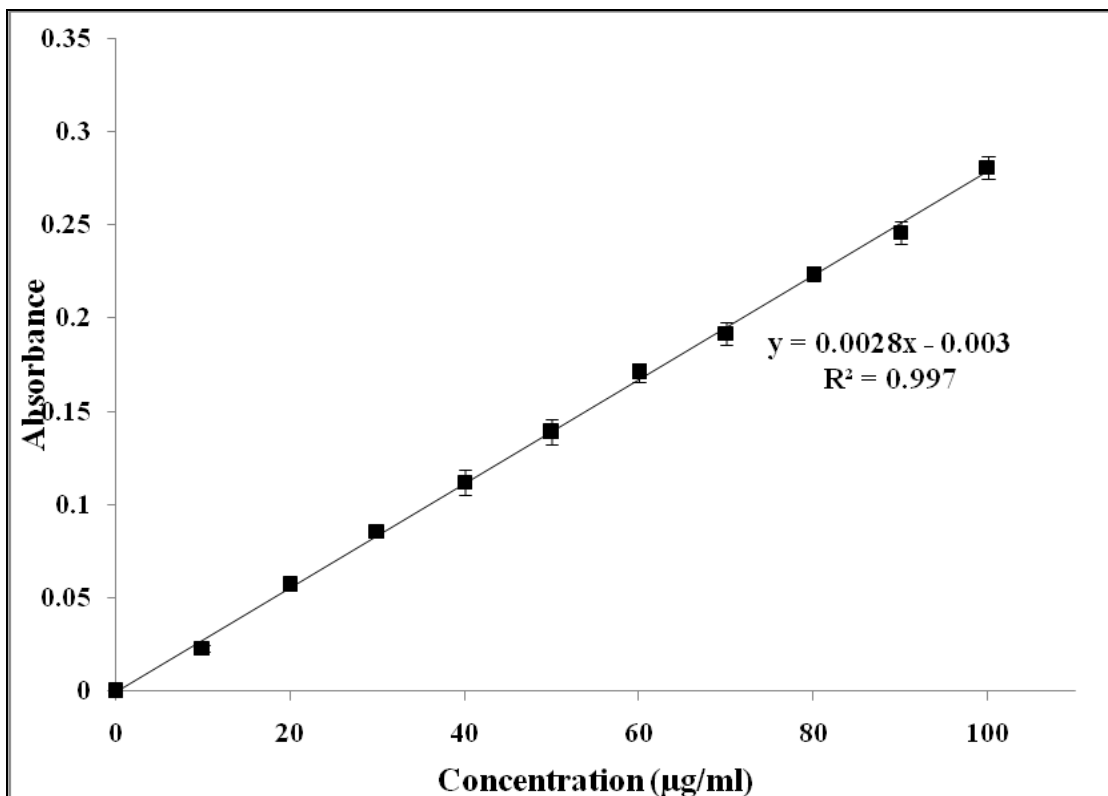


Figure 4.2. Standard curve of CA in ethyl acetate.

4.3. $^1\text{H-NMR}$

$^1\text{H-NMR}$, an acceptable tool with great promise, is routinely used to characterize the mixtures of organic compounds and their chemical compatibility (Forseth and Schroeder, 2011; Stark *et al.*, 2016). Change in shift, appearance of new proton, deletion of existing proton indicates the incompatibility between compounds (Stark *et al.*, 2016). In this study, the $^1\text{H-NMR}$ spectra of CA, PLGA, and CA-PLGA mixture were shown in Figure 4.3., where the signal is plotted on the y axis and the frequency on the x axis. The $^1\text{H-NMR}$ spectra of CA (Figure 4.3.a) and PLGA (Figure 4.3.b) confirmed their structural identities. On the other hand, $^1\text{H NMR}$ spectra of CA-PLGA mixture did not exhibit the appearance of any new peak of proton or any

change in shift or any change in peak pattern (Figure 4.3.c), which revealed the chemical compatibility between CA and PLGA.

4.4. FTIR

FTIR studies provide information about the stability of the formulation, as well as the interaction between drugs and the excipients in the formulation (Gaonkar *et al.*, 2017). Each compound has its own characteristic FTIR peaks due to presence of different co-valent bonds (Lu *et al.*, 2018). According to vibrational spectroscopy, each bond has its own vibrational energy, which is unique, and thus helps to distinguish one component from other (Lu *et al.*, 2018). In this study, FTIR spectra were recorded for CA, PLGA, TPGS, a physical mixture of CA, PLGA and TPGS, and CA nanoparticles (Figure 4.4.), where the transmittance is plotted on the y axis and the wavenumber is on the x axis. From this FTIR results it can be seen, that the spectra showed the characteristic peaks of CA at 1648.04 cm^{-1} , is due to the presence of carbonyl group and bonds above 3590 cm^{-1} depicting the presence of hydroxyl functional group (Figure 4.4.a). The FTIR spectrum of PLGA revealed the characteristic peaks at 3618.53 cm^{-1} for hydroxyl function, 2997.72 cm^{-1} for C-H stretching bands, and 1744.63 cm^{-1} for C-O stretching band of ester (Figure 4.4.b). In the FTIR spectrum of TPGS, the peak shown at 3424.26 cm^{-1} is indicating the presence of terminal hydroxyl function while those at 2871.26 cm^{-1} and 1742.75 cm^{-1} indicate the $-\text{CH}$ and carbonyl function stretching (Figure 4.4.c). Most of the characteristic peaks of CA, PLGA and TPGS appeared in the FTIR spectrum of the physical mixture without any major change in peak position or intensity (Figure 4.4.d). Similarly in CA nanoparticles, the presence of the characteristic peaks of the CA and excipients indicates the presence of CA in native form without any chemical interaction with the polymer and emulsifier (Figure 4.4.e).

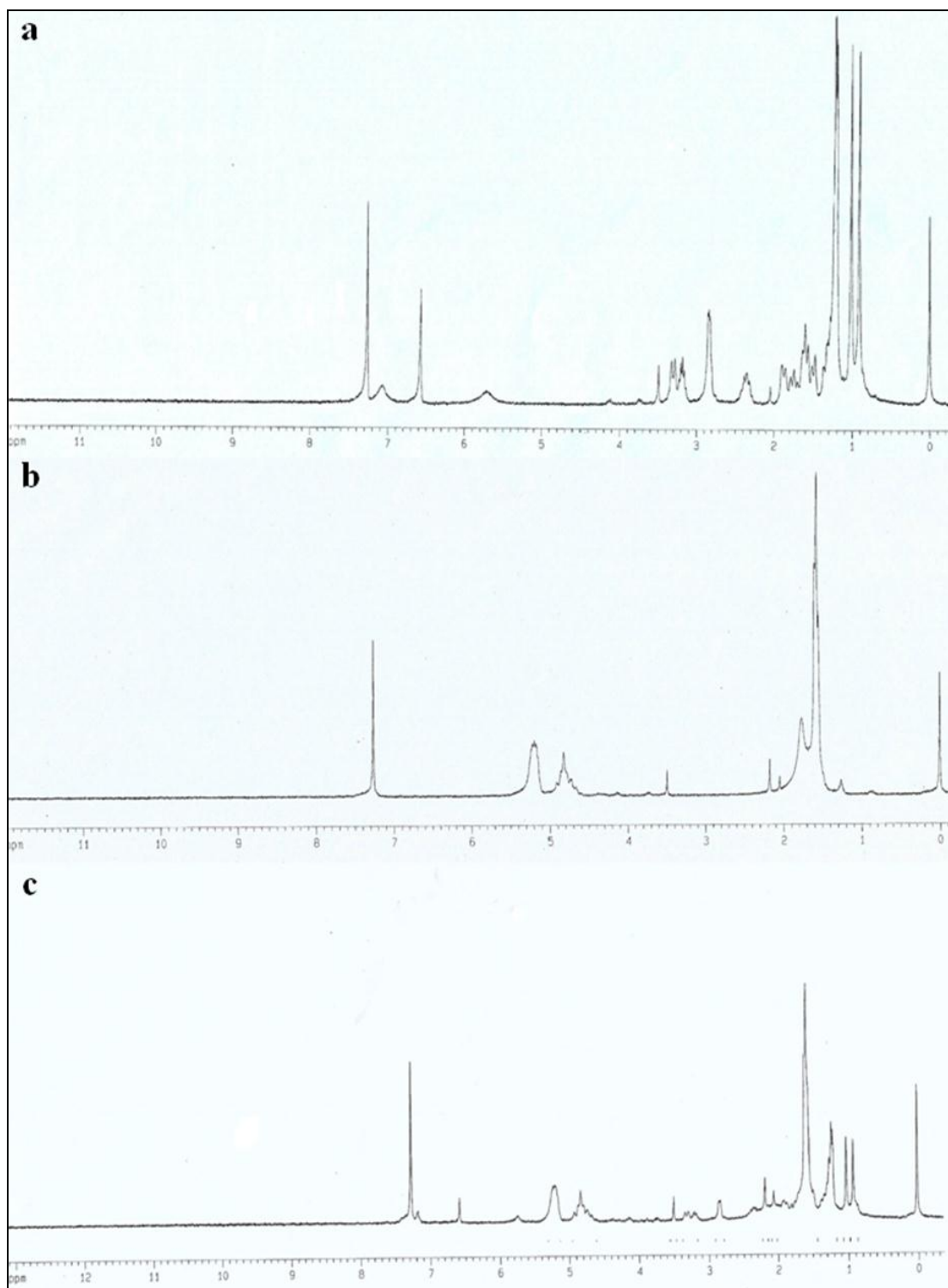


Figure 4.3. ^1H -NMR spectra of CA (a), PLGA (b), and CA-PLGA (c) mixture in CDCl_3 .

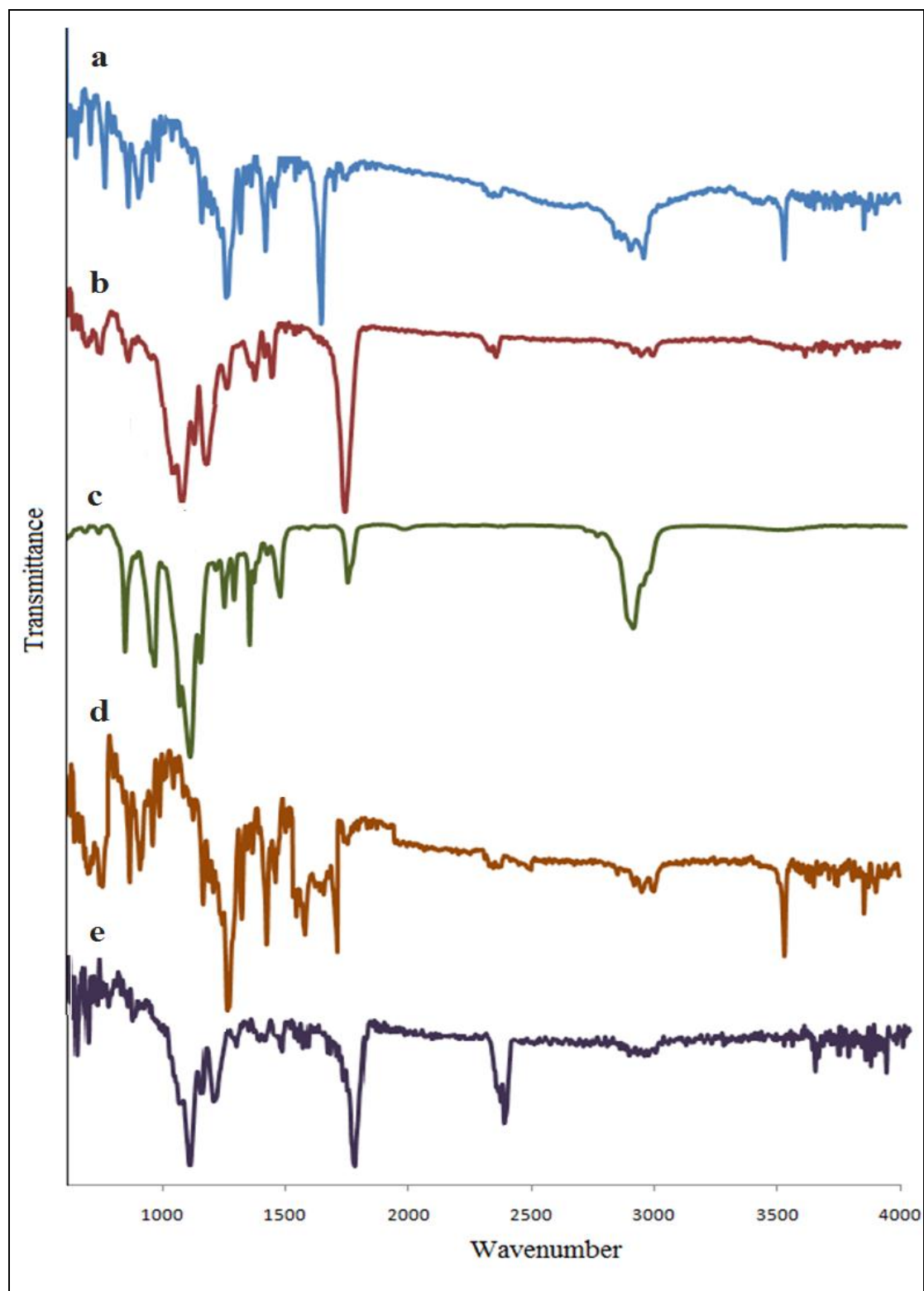


Figure 4.4. FTIR of CA (a), PLGA (b), TPGS (c), CA-PLGA-TPGS mixture (d), CA nanoparticles (e).

4.5. Thermal analysis by DSC

DSC is a thermo analytical technique in which the difference in the amount of heat required to increase the temperature of a sample is measured (Chiu *et al.*, 2011). The DSC thermograms of CA, PLGA, their physical mixture, and CA nanoparticles are shown in Figure 4.5., where the x axis represents change of temperature with time and y axis represents heat flow. The thermograms consist of descending peaks, which means the thermal analysis process was endothermic (Chiu *et al.*, 2011). Free CA and PLGA showed sharp endothermic peaks at 191.58°C (Figure 4.5.a) and 41.59°C (Figure 4.5.b), respectively. It was reported that the melting point of CA was 185 to 190°C (Das *et al.*, 2018) and melting point of PLGA (75:25) polymer is above 37°C (Makadia *et al.*, 2011). In the physical mixture the PLGA remained almost unchanged (38.28°C) and CA also remained almost unchanged (190.91°C) as evident from the DSC thermogram (Figure 4.5.c). This indicates that there was no reaction between the drug and the polymer. The absence of characteristic melting peak of CA in the DSC thermogram of CA nanoparticles may be due to the conversion of CA from the crystalline state to the amorphous state or disordered crystalline state during nanoformulation which inhibited crystal growth thereby leading to enhanced stability of the formulation (Figure 4.5.d). The endothermic peak at 43.04°C (Figure 4.5.d) shows that the value is close to that of free polymer, which means the polymer is not degraded in formation. The peak temperatures of the components are mentioned in Table 4.1.

Table 4.1. Endothermic peak temperatures of different components.

Compound	Endothermic peak temperature
Free CA	191.58°C
PLGA	41.59°C
Mixture of CA and PLGA	38.28°C, 190.91°C
Nanoparticle	43.04°C

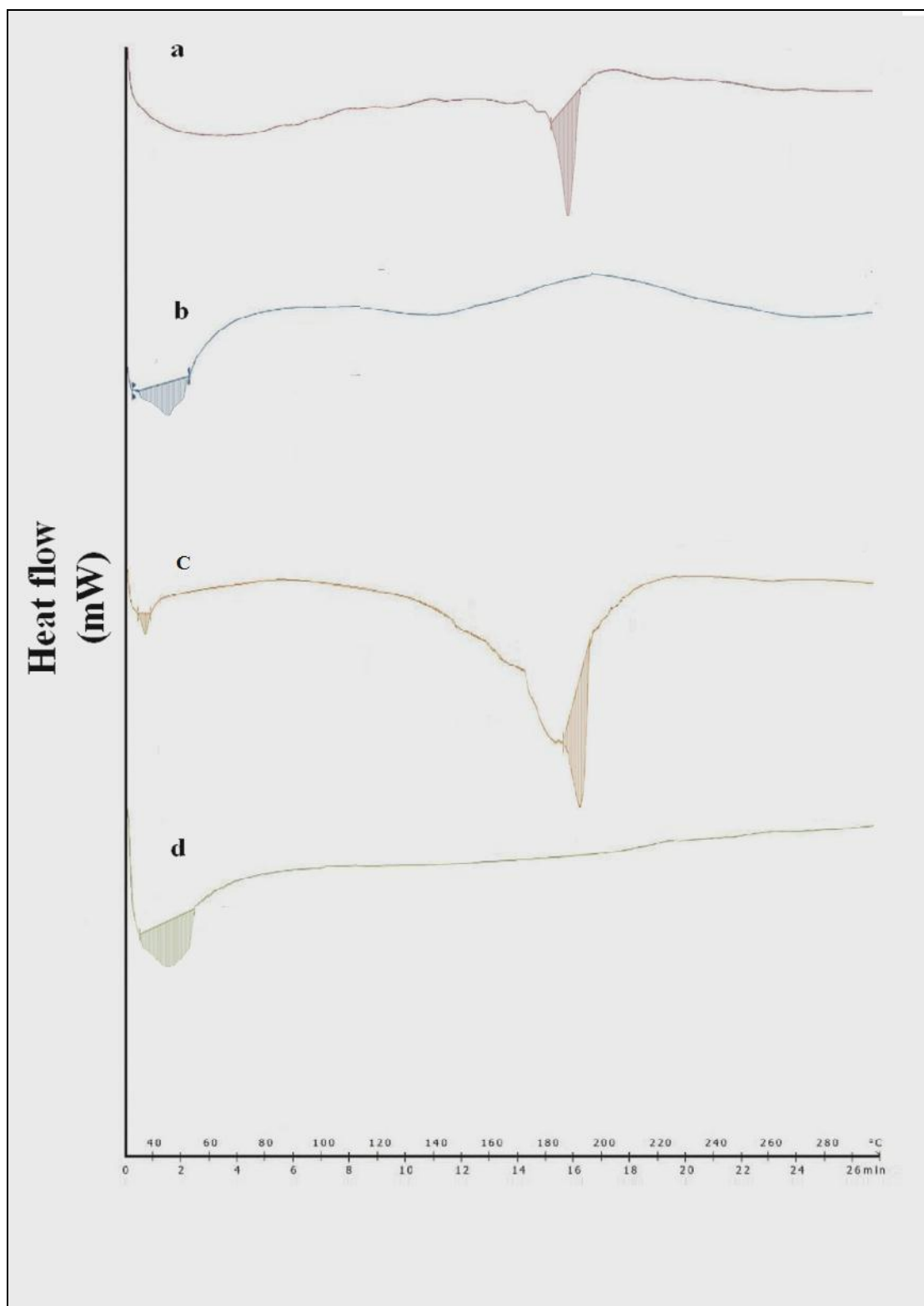


Figure 4.5. DSC thermogram of CA (a), PLGA (b), CA-PLGA mixture (c), and CA nanoparticles (d).

4.6. Crystallinity evaluation by XRD

XRD analysis detects the presence of crystalline property of samples; amorphous materials, like polymers, do not produce sharp diffraction peaks, whereas sharp peak with high intensity is found in XRD of crystalline materials (Bunaciu *et al.*, 2015). The XRD patterns of CA, PLGA, their physical mixture, and CA nanoparticles are shown in Figure 4.6., where the x axis represents intensity (cps) and y axis represents 2θ values. The peaks for free CA found to be free of distortion and have high intensity, which indicates that the free CA is crystalline nature in nature (Figure 4.6.a). In previous investigations also CA was reported to be solid crystals (Das *et al.*, 2018). The absence of peaks in the XRD pattern for PLGA confirmed its amorphous nature (Figure 4.6.b) Minor reference peaks could be lost in the background noise, so it may be acceptable if they are not observed (Bunaciu *et al.*, 2015). In journal report PLGA was mentioned as an amorphous compound (Gentile *et al.*, 2014). The physical mixture of CA and PLGA exhibited a number of distinct peaks; however the positions of the peaks were somewhat different from those in CA suggesting that minor interactions occurred between CA molecules and the polymer matrix (Figure 4.6.c). The disappearance of distinct peaks in CA nanoparticles suggested the conversion of crystalline state to amorphous state during nanoparticles formulation (Figure 4.6.d). The highest intensity values of the components are mentioned in Table 4.2.

Table 4.2. Highest intensity values of different components.

Compound	Highest intensity (cps)
Free CA	3830.495
PLGA	745.416
Mixture of CA and PLGA	3810.314
Nanoparticle	750.168

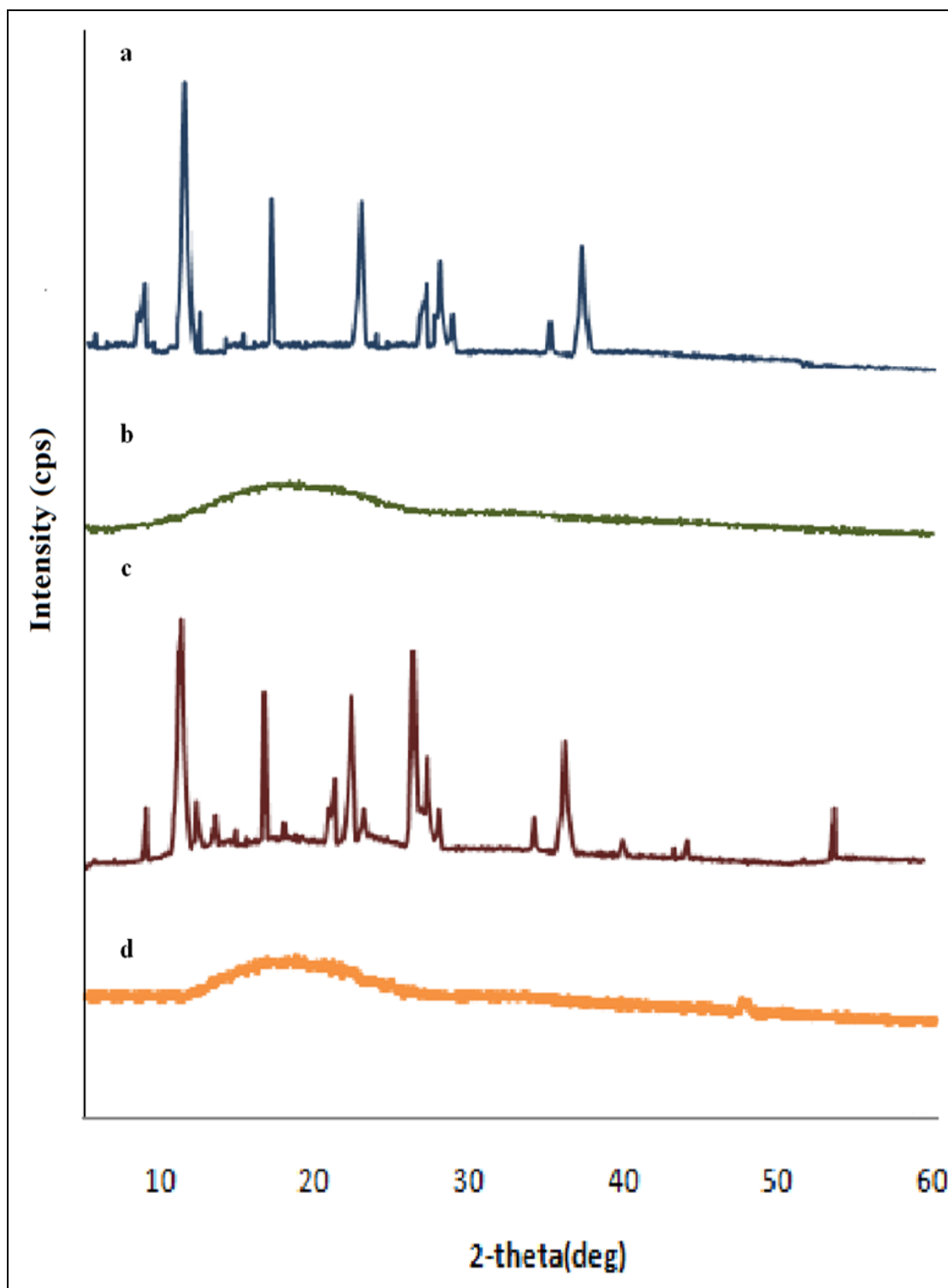


Figure 4.6. XRD of CA (a), PLGA (b), CA-PLGA (c), and CA nanoparticles (d).

4.7. NY, DL and EE

The amount of CA enloaded in the nanoparticles was determined by spectroscopic measurements at 279 nm. DL amounts and EE of various CA loaded nanoparticle

formulations prepared by varying the amount of CA and PLGA were measured. The highest DL content of CA in CA loaded PLGA nanoparticle was detected as $8.97 \pm 0.43\%$. EE was detected as $65.69 \pm 3.8\%$. In an experiment, Insulin loaded nanoparticles with EE of about 70% was proved to be effective in insulin delivery (Wu *et al.*, 2017). Another report claims to have good anticancer activity of anticancer drug loaded nanoparticles having DL $9.25 \pm 2.8\%$ (Gaonkar *et al.*, 2017). Based on these reports it can be used for therapeutic approaches. So, it can be said that, CA was encapsulated into vitamin E TPGS emulsified PLGA nanoparticle with a relatively high DL capacity and EE, which might be due to the strong interaction between CA and polymer. Highest NY of CA nanoparticles was $66.54 \pm 4.4\%$ DL and EE percentages are shown in Table 4.1. The comparison between different drug-polymer ratios is shown in Figure 4.7. Comparing the percentages of NY, DL and EE of CA nanoparticles with varying drug-polymer ratios (1:6.66, 1:10.00 and 1:20.00) it was observed that taking polymer ten times to the drug quantity will yield maximum nanoparticles with good drug entrapment.

Table 4.3. NY, DL and EE percentages of different drug-polymer ratio.

Drug-polymer ratio	Weight of formulated nanoparticles (mg)	NY (%)	DL (%)	EE (%)
1:6.66	35.85 ± 2.35	62.34 ± 4.2	4.22 ± 0.84	20.19 ± 2.1
1:10.00	36.6 ± 3.22	66.54 ± 4.4	8.97 ± 0.43	65.69 ± 3.8
1:20.00	31.5 ± 2.08	60.00 ± 3.9	6.76 ± 0.87	85.18 ± 4.7

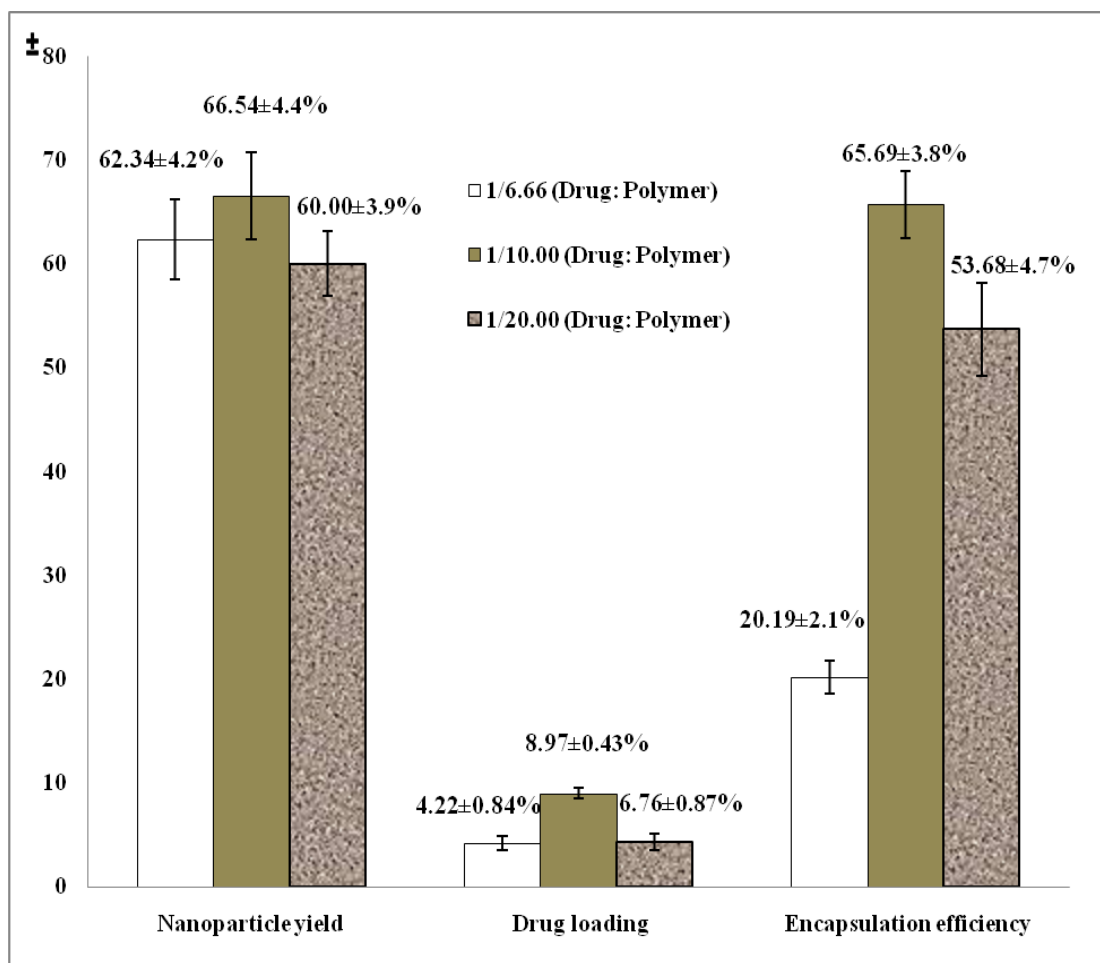


Figure 4.7. Comparison between NY, DL, and EE in different drug-polymer ratio.

4.8. TEM

The TEM image showed (Figure 4.8.) a discrete spherical outline and monodispersed size distribution of nanoparticles and measured its size around 53.3 ± 7.2 nm. Before more than a decade, most of the clinically approved anticancer nanoparticles have size ranging from 100 to 200 nm (Gradishar *et al.*, 2005). But recent studies showed that anticancer drug enloaded nanoparticles with smaller sizes exhibited better effects *in vivo*, such as greater tissue penetration provides enhanced tumor inhibition, particularly those with size around or smaller than 50 nm (Cabral *et al.*, 2011). Another report says, nanoparticles in the size range 1-100 nm are accepted to be therapeutically active for cancer (Davis *et al.*, 2008). In many tumors, nanoparticles larger than 60 nm in diameter are not able to effectively penetrate the collagen membrane of tumors (Jain *et al.*, 2010). So, the size of CA nanoparticles determined

by TEM analysis can be considered as acceptable size and can be further used for therapeutic approaches

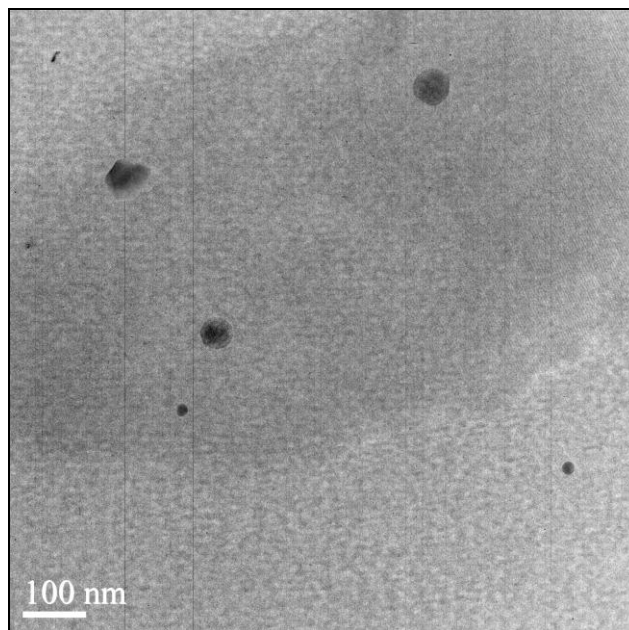


Figure 4.8. TEM image of CA nanoparticles.

4.9. AFM

The AFM helps in determination of parameters like amplitude or height parameters, functional or statistical parameters and spatial parameters; it also allows the topographic characterization of surfaces at resolutions (Last et al., 2010). AFM studies confirmed the smooth and spherical surface of the nanoparticles along with the absence of aggregation or adhesion between the nanoparticles (Figure 4.9.b), three dimensional image (Figure 4.9.a) revealed smooth spherical topography with homogeneous size distribution (Figure 4.9.). The size height and length profile of CA nanoparticles is shown in (Figure 4.9.c). As it was discussed earlier, that the smaller size ($\leq 50\text{nm}$) of nanoparticles are proved to be useful in anticancer treatments (Cabral *et al.*, 2011), CA nanoparticles having size below 50nm according to the AFM results, are also expected to be effective in drug delivery.

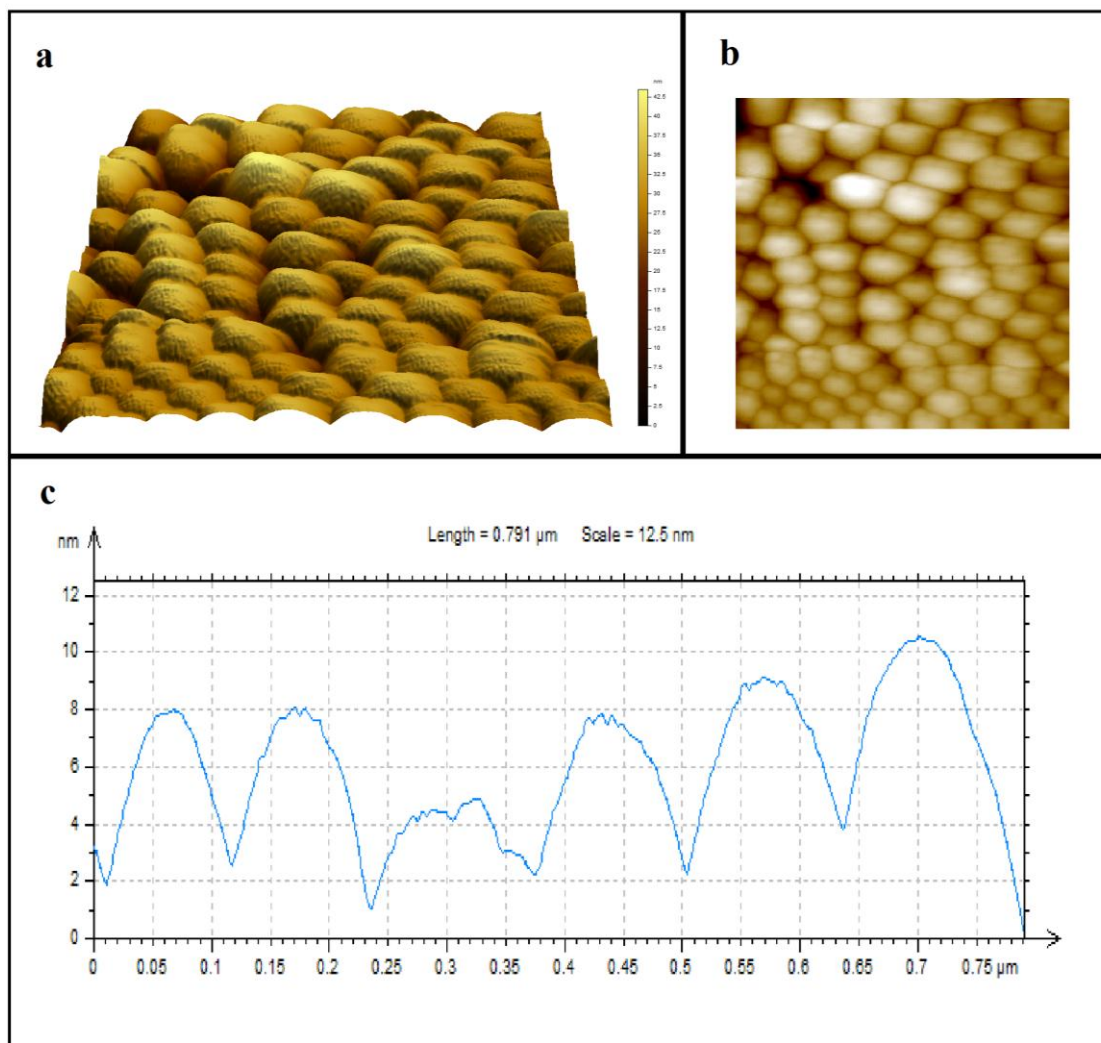


Figure 4.9. AFM image of CA nanoparticle: Three-dimensional view (a), topographical image (b) and surface height and length profile (c).

4.10. DLS

DLS study also analyses the size of nanoparticles. This DLS study reveals that the average diameter of nanoparticles was calculated to be 103.9 ± 27.06 nm and the polydispersity index was found to be 0.191 (Figure 4.10.). The size determined by the DLS method was found higher than that of TEM (Figure 4.8.) and AFM (Figure 4.8.) studies. In microscopic methods the size parameters are determined exactly from the original surface of the nanoparticle whereas in DLS the light beam scatters from the stagnant solvent layer adhered to its surface, thus the size determined includes the thin film of solvent (Mizuta *et al.*, 2019).

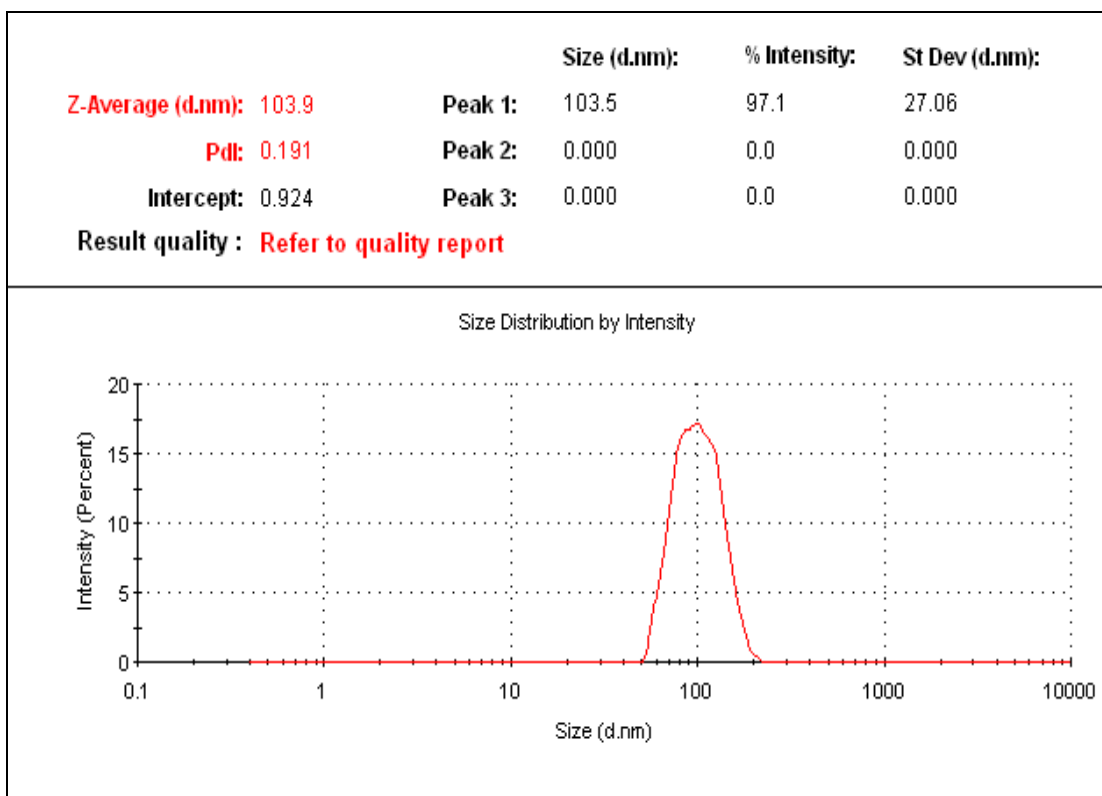


Figure 4.10. Particle size distribution pattern of CA nanoparticles.

4.11. Surface charge

Zeta potential value of CA nanoparticle is -26.7 ± 6.95 mV (Figure 4.11.). Value of zeta potential smaller than -15 mV means the nanoparticles start to agglomerate, while higher than -30 mV shows enough bilateral repulsion and colloidal stability (Blanco *et al.*, 2018). Nanoparticles having zeta potential between -10 and $+10$ mV are reported as neutral in nature, on the other hand those with zeta potential values of greater than $+30$ mV or less than -30 mV are reported as strongly cationic and strongly anionic, respectively; as maximum cellular membranes are negatively charged, nanoparticles with negative zeta potential value will be able to permeate cellular membrane but nanoparticles with positive zeta potential value will struggle to permeate cellular membrane as well as cause toxicity (Clogston & Patri, 2011). Considering the aforementioned literature, it would be predicted that the developed CA nanoparticles may be stable.

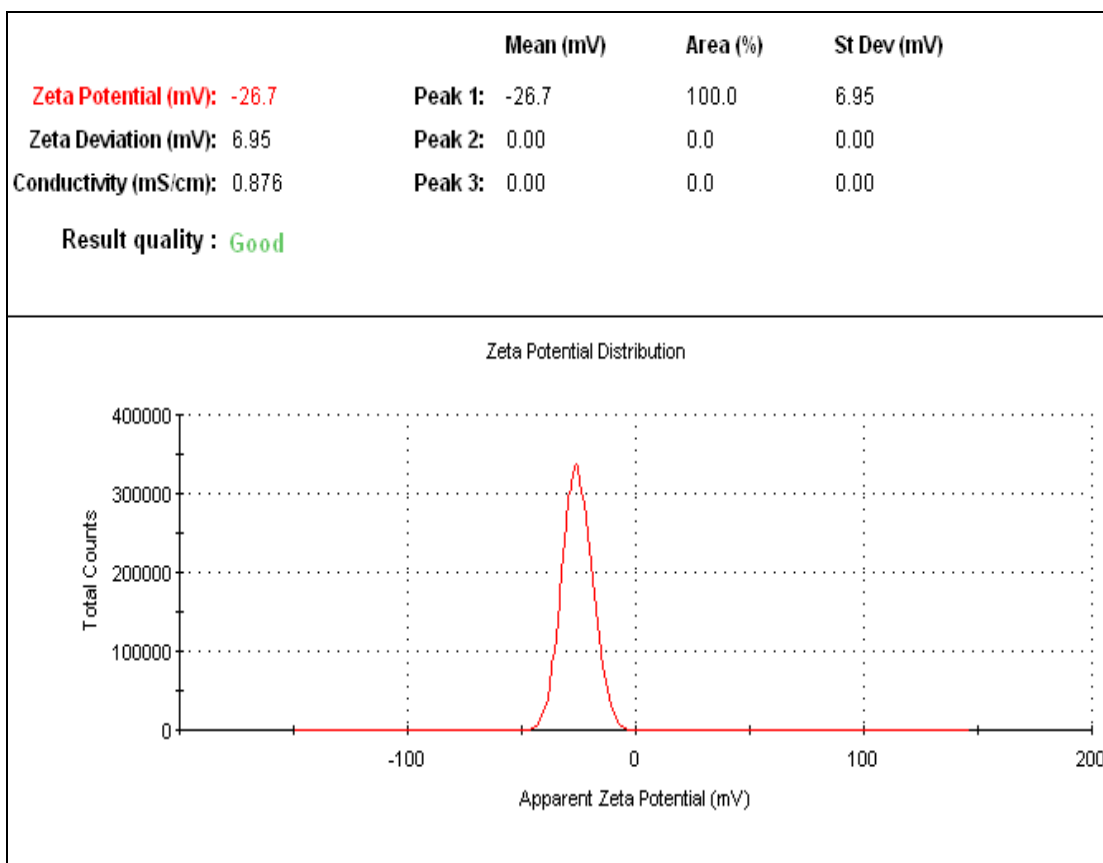


Figure 4.11. zeta potential distribution profile of CA nanoparticles.

4.12. Standard curve of CA in PBS

Standard curve is based on the principle of Beer-Lambert's law, which states that, the quantity of light absorbed by a substance dissolved in a fully transmitting solvent is directly proportional to the concentration of the substance and the path length of the light through the solution (Baker et al., 2014) Plotting standard curve of a compound dissolved in a certain solvent helps in the determination of unknown concentration of the solution of that compound (Dastidar & Sa, 2009). The standard curve of CA in PBS follows linearity (Figure 4.12.) and bears equation: $y = 0.004x$ (where x =concentration and y = absorbance) and have R^2 value 0.999. This equation shows that the increase in concentration of PBS solution of CA is directly proportional to the increase of absorbance values.

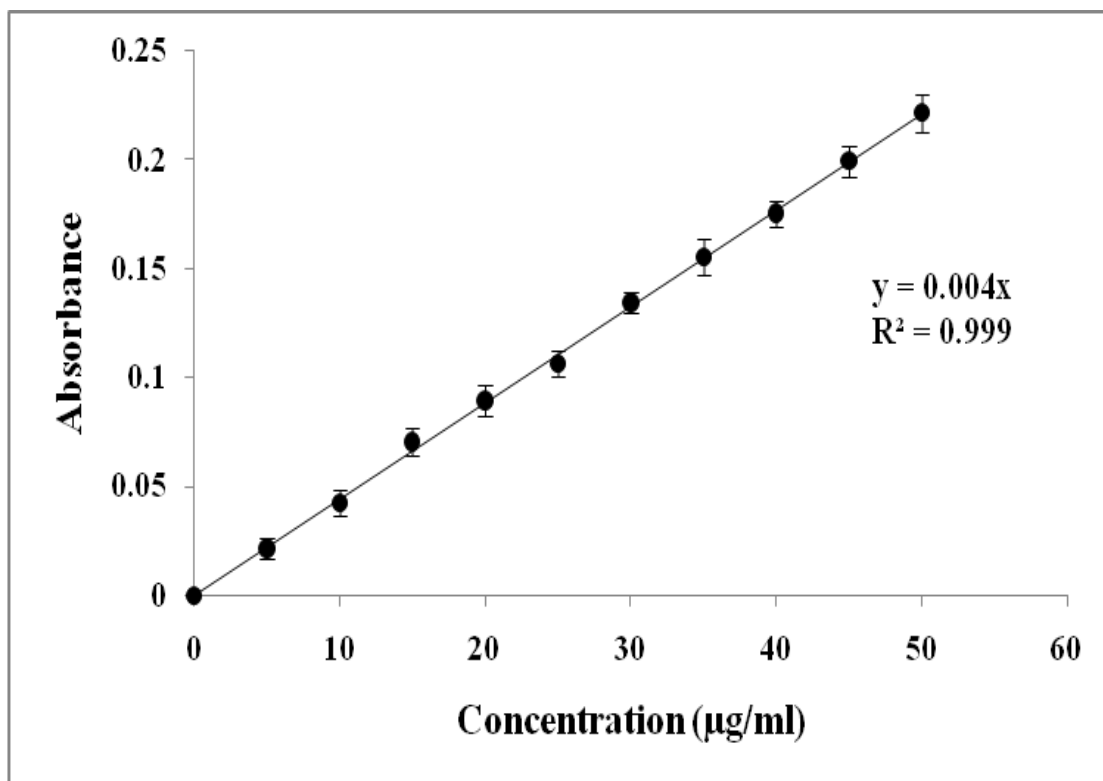


Figure 4.12. Standard curve of CA in PBS.

4.13. *In vitro* drug release study

Initial release was 41.2% observed within first 30 min (Figure 4.12.). Initial release with high percentage of drug release may take place if some unincorporated drug particles were loosely attached to polymeric shell surface (Gaonkar *et al.*, 2017). The release was moderate up to 10 hrs; this was followed by a slower sustained release. The property of long duration release of drug makes nanoparticles act like drug depot, which exhibits prolonged release kinetics and long persistence at the target site (Guzman *et al.*, 1996). Around 98.13% of CA was released from nanoparticulated formulation over the period of 4 days. The sustained release occurred due to the diffusion, swelling or erosion and degradation of the polymeric matrix in PBS, as PLGA is soluble in aqueous buffers (Makadia *et al.*, 2011). *In vitro* drug release from nanoparticles prepared by nanoprecipitation generally occurs in two steps (Wang and Tan, 2016). At first, the burst release takes place, due to the adhesion of drug substances on the nanoparticle surface and then prolonged release starts (Wang and Tan, 2016).

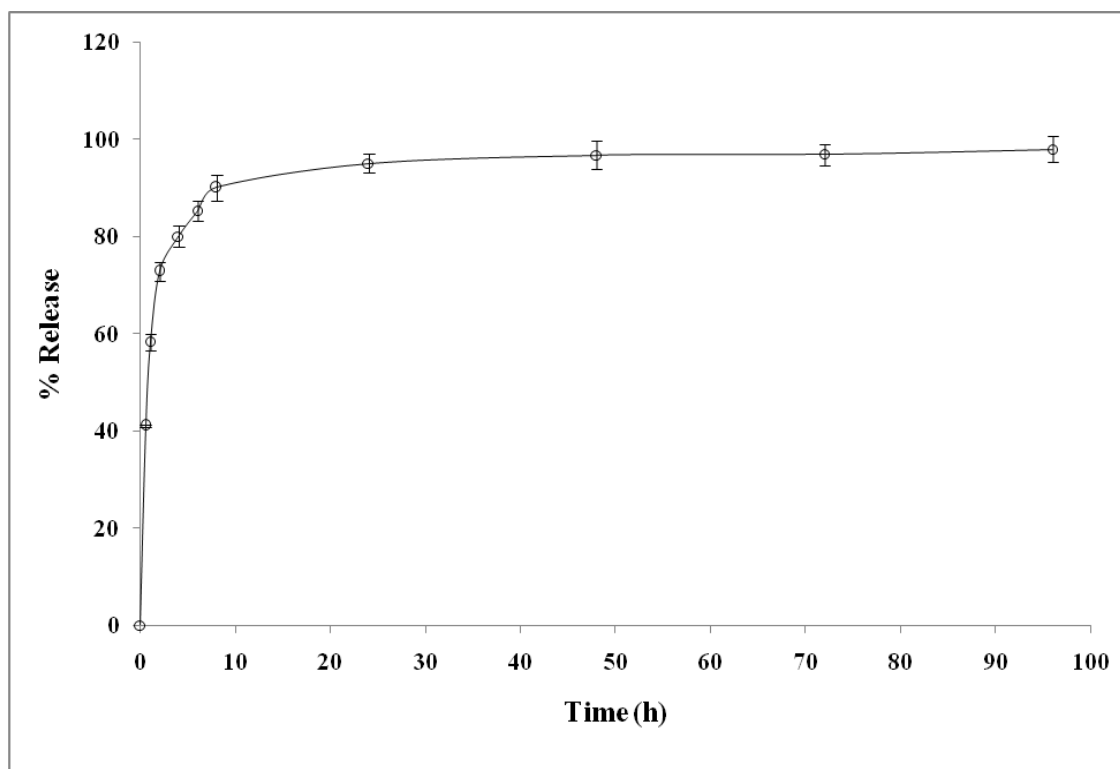


Figure 4.13. Cumulative percent of *in vitro* release of CA from nanoparticles.

Chapter 5

Conclusion

5. Conclusion

From the reports of different journals it was found that CA possesses anticancer, antihyperlipidemic, antidiabetic, antioxidant, anti-inflammatory, hepatoprotective and antimicrobial properties. But due to its hydrophobic nature, it was reported to have low bioavailability. On reviewing more reports, it has been found that therapeutically active compounds can be delivered encapsulated in polymeric nanoparticle. The CA-loaded PLGA nanoparticles were prepared by using vitamin E TPGS as an emulsifier by nanoprecipitation method the nanoparticle yield, loading of drug in polymeric nanoshell and encapsulation efficiency found to be significant. The mean size and surface charge of CA nanoparticles was found to be favourable in drug delivery and cell membrane penetration. Beside, the results of physicochemical characterizations of CA, PLGA, TPGS, physical mixture of CA, PLGA and TPGS and CA nanoparticles showed that free CA is compatible with excipients and its physicochemical properties were not affected. The *in vitro* drug release study was also found productive. A sustained release of entrapped drug over a period of 96 h was observed. Therefore, it may be claimed that CA nanoparticles would be a potential formulation for subjecting to pre-clinical studies to evaluate their therapeutic efficacy over conventional formulation of CA and free CA.

References

References

- Allemann E, Gurny R, Doekler E. Drug-loaded nanoparticles preparation methods and drug targeting issues. *Eur J Pharm Biopharm.* 1999;39:173-9.
- Alshamsan A. Nanoprecipitation is more efficient than emulsion solvent evaporation method to encapsulate cucurbitacin I in PLGA nanoparticles. *Saudi Pharm J.* 2014;22:219-22.
- Andon FT, Fadeel B. Programmed cell death: molecular mechanisms and implications for safety assessment of nanomaterials. *Acc Chem Res.* 2013;46:733-42.
- Bahri S, Jameleddine S, Shlyonsky V. Relevance of carnosic acid to the treatment of several health disorders: molecular targets and mechanisms. *Biomed Pharmacother.* 2016;84:569-82.
- Baker WB, Parthasarathy AB, Busch DR, Mesquita RC, Greenberg JH, Yodh AG. Modified Beer-Lambert law for blood flow. *Biomed Opt Express.* 2014;5:4053-75.
- Baliga, MS, Jimmy R, Thilakchand KR, Sunitha V, Bhat NR, Saldanha E, Rao S, Rao P, Arora R, Palatty PL. *Ocimum Sanctum* L. (Holy Basil or Tulsi) and its phytochemicals in the prevention and treatment of cancer. *Nutr Cancer.* 2013;65:26-35.
- Bhattacharya S, Mondal L, Mukherjee B, Dutta L, Ehsan I, Debnath MC, Gaonkar RH, Pal MM, Majumdar S. Apigenin loaded nanoparticle delayed development of hepatocellular carcinoma in rats. *Nanomedicine.* 2018;14:1905-17.
- Birtic S, Dussort P, Pierre FX, Bily AC, Roller M. Carnosic acid. *Phytochemistry.* 2015;115:9-19.
- Blanco A, Monte MC, Campano C, Balea A, Merayo N, Negro C. Nanocellulose for Industrial Use: Cellulose Nanofibers (CNF), Cellulose Nanocrystals (CNC), and Bacterial Cellulose (BC). In *Handbook of Nanomaterials for Industrial Applications*; Elsevier: Amsterdam, The Netherlands, 2018; pp.74-126
- Borrás-Linares I, Pérez-Sánchez A, Lozano-Sánchez J, Barrajón-Catalán E, Arráez-Román D, Cifuentes A, Micol V, Carretero AS. A bioguided identification of the active compounds that contribute to the antiproliferative/cytotoxic effects of rosemary extract on colon cancer cells. *Food Chem Toxicol.* 2015;80:215-22.

- Brieskorn CH, Fuchs A, Bredenberg JB, McChesney JD, Wenkert E. The structure of carnosol. *J Org Chem.* 1964;29:2293-8.
- Brieskorn, CH, Dumling HJ. Carnosolsaure, der wichtigeantioxydativwirksame Inhaltsstoff des Rosmarin-und Salbeiblattes. *Eur Food Res Tech Z. Lebensm Unters Forsch.* 1969;141:10-6.
- Bunaciu AA, Udriștioiu EG, Aboul-Enein HY. X-ray diffraction: instrumentation and applications. *Crit Rev Anal Chem.* 2015;45:289-99.
- Cabral H, Matsumoto Y, Mizuno K, Chen Q, Murakami M, Kimura M, Terada Y, Kano MR, Miyazono K, Uesaka M, Nishiyama N, Kataoka K. Accumulation of sub-100 nm polymeric micelles in poorly permeable tumours depends on size. *Nat Nanotechnol.* 2011; 6:815-23.
- Chen R, Huo L, Shi X, Bai R, Zhang Z, Zhao Y, Chang Y. Endoplasmic reticulum stress induced by zinc oxide nanoparticles is an earlier biomarker for nanotoxicological evaluation. *ACS Nano.* 2014;8:2562-74.
- Chen Y, Zou C, Mastalerz M, Hu S, Gasaway C, Tao X. Applications of micro-fourier transform infrared spectroscopy (FTIR) in the geological sciences-a review. *Int J Mol Sci.* 2015;18;16:30223-50.
- Chidambaram M, Krishnasamy K. Drug-Drug/Drug-Excipient Compatibility Studies on Curcumin using Non-Thermal Methods. *Adv Pharm Bull.* 2014;4:309-12.
- Chien PJ, Suzuki T, Tsujii M, Ye M, Minami I, Toda K, Otsuka H, Toma K, Arakawa T, Araki K, Iwasaki Y, Shinada K, Ogawa Y, Mitsubayashi K. Biochemical gas sensors (biosniffers) using forward and reverse reactions of secondary alcohol dehydrogenase for breath isopropanol and acetone as potential volatile biomarkers of diabetes mellitus. *Anal Chem.* 2017;89:12261-8.
- Chiu MH, Prenner EJ. Differential scanning calorimetry: an invaluable tool for a detailed thermodynamic characterization of macromolecules and their interactions. *J Pharm Bioallied Sci.* 2011;3:39-59.
- Choudhury H, Gorain B, Pandey M, Kumbhar SA, Tekade RK, Iyer AK, Kesharwani P. Recent advances in TPGS-based nanoparticles of docetaxel for improved chemotherapy. *Int J Pharm.* 2017;529:506-22.
- Clogston JD, Patri AK. Zeta potential measurement. *Methods Mol Biol.* 2011;697:63-70.

- Cruz LJ, Tacken PJ, Fokkink R, Joosten B, Stuart MC, Albericio F, Torensma R, Figdor CG. Targeted PLGA nano- but not microparticles specifically deliver antigen to human dendritic cells via DC-SIGN *in vitro*. *J Control Release*. 2010;144:118-26.
- Danhier F, Ansorena E, Silva JM, Coco R, Breton AL, Preat V. PLGA-based nanoparticles: An overview of biomedical applications. *J Control Release*. 2012;161:505-22.
- Das S, Joardar S, Manna P, Dua TK, Bhattacharjee N, Khanra N, Khanra R, Bhowmick S, Kalita J, Saha A, Ray S, De Feo V, Dewanjee S. Carnosic acid, a natural diterpene, attenuates arsenic-induced hepatotoxicity via reducing oxidative stress, MAPK activation, and apoptotic cell death pathway. *Oxid Med Cell Longev*. 2018;2018:1421-38
- Dastidar DG, Sa B. A comparative study of UV-spectrophotometry and first-order derivative UV-spectrophotometry methods for the estimation of diazepam in presence of Tween-20 and propylene glycol. *AAPS PharmSciTech*. 2009;10:1396-400.
- Davis ME, Chen ZG, Shin DM. Nanoparticle therapeutics: An emerging treatment modality for cancer. *Nat Rev Drug Discov*. 2008;7:771-82.
- De Assis DN, Mosqueira VC, Vilela JM, Andrade MS, Cardoso VN. Release profiles and morphological characterization by atomic force microscopy and photon correlation spectroscopy of 99m Technetium—fluconazole nanocapsules. *Int J Pharm*. 2008;349:152-60.
- Dickmann LJ, VandenBrink BM, Lin YS. *In vitro* hepatotoxicity and cytochrome P450 induction and inhibition characteristics of carnosic acid, a dietary supplement with antiadipogenic properties. *Drug Metab Dispos*. 2012;40:1263-7.
- Diebold Y, Calonge M. Applications of nanoparticles in ophthalmology. 2010;29:596-609.
- Ding SM, Zhang ZH, Song J, Cheng XD, Jiang J, Jia XB. Enhanced bioavailability of apigenin via preparation of a carbon nanopowder solid dispersion. *Int J Nanomedicine*. 2014;9:2327-33.

- Doolaage EH, Raes K, De Vos F, Verhé R, De Smet S. Absorption, distribution and elimination of carnosic acid, a natural antioxidant from *Rosmarinus officinalis*, in rats. *Plant Foods Hum Nutr.* 2011;66:196-202.
- El-shabouri MH. Positively charged nano particles for improving the oral bioavailability of cyclosporine-A. *Int J Pharm.* 2002;249:101-8.
- Ezzat HM, Elnaggar YSR, Abdallah OY. Improved oral bioavailability of the anticancer drug catechin using chitosomes: design, *in-vitro* appraisal and *in-vivo* studies. *Int J Pharm.* 2019;565:488-98.
- Feng SS, Mu L, Chen BH, Pack DW. Polymeric nanospheres fabricated with natural emulsifiers for clinical administration of an anticancer drug paclitaxel (Taxol). *Mater Sci Eng C.* 2002;20:85-92.
- Fessi H, Puisieux F, Devissaguet JP, Ammoury N, Benita S. Nanocapsule formation by interfacial deposition following solvent displacement. *Int J Pharm.* 1989;55:R1-R4.
- Forseth RR, Schroeder FC. NMR-spectroscopic analysis of mixtures:from structure to function. *Curr Opin Chem Biol.* 2011;15:38-47.
- Gao Q1, Liu H, Yao Y, Geng L, Zhang X, Jiang L, Shi B, Yang F. Carnosic acid induces autophagic cell death through inhibition of the Akt/mTOR pathway in human hepatoma cells. *J Appl Toxicol.* 2015;35:485-92.
- Gao X, Cui Y, Levenson RM, Chung LWK, Nie S. In-vivo cancer targeting and imaging with semiconductor quantum dots. *Nat Biotechnol.* 2004;22:969–76.
- Gaonkar RH, Ganguly S, Dewanjee S, Sinha S, Gupta A, Ganguly S, Chattopadhyay D, Debnath, M. Garcinol loaded vitamin E TPGS emulsified PLGA nanoparticles: preparation, physicochemical characterization, *in vitro* and *in vivo* studies. *Sci Rep.* 2017;3:7:530
- Garinot M, Fiévez V, Pourcelle V, Stoffelbach F, des Rieux A, Plapied L, Theate I, Freichels H, Jérôme C, Marchand-Brynaert J, Schneider YJ, Préat V. PEGylated PLGA-based nanoparticles targeting M cells for oral vaccination. *J Control Release.* 2007;120:195-204.
- Gaya M, Repetto V, Toneatto J, Anesini C, Piwien-Pilipuk G, Moreno S. Antiadipogenic effect of carnosic acid, a natural compound present in *Rosmarinus officinalis*, is

- exerted through the C/EBPs and PPAR γ pathways at the onset of the differentiation program. *Biochim Biophys Acta*. 2013;1830:3796-806.
- Gazi U, Martinez-Pomares L. Influence of the mannose receptor in host immune responses, *Immunobiology*. 2009;214:554-61.
- Gentile P, Chiono V, Carmagnola I, Hatton PV. An overview of poly(lactic-co-glycolic) acid (PLGA)-based biomaterials for bone tissue engineering. *Int J Mol Sci*. 2014; 15:3640-59.
- Gómez G, Pikal MJ, Rodríguez-Hornedo N. Effect of initial buffer composition on pH changes during far-from-equilibrium freezing of sodium phosphate buffer solutions. *Pharm Res*. 2001;18:90-7.
- Gradishar WJ, Tjulandin S, Davidson N, Shaw H, Desai N, Bhar P, Hawkins M, O'Shaughnessy J. Phase III trial of nanoparticle albumin-bound paclitaxel compared with polyethylated castor oil-based paclitaxel in women with breast cancer. *J Clin Oncol*. 2005;23:7794-803.
- Guarneri V, Dieci MV, Conte P. Enhancing intracellular taxane delivery: current role and perspectives of nanoparticle albumin-bound paclitaxel in the treatment of advanced breast cancer. *Expert Opin Pharmacother*. 2012;13:395-406.
- Guerrero IC, Andres LS, Leon LG, Machin RP, Padron JM, Luis JG, Delgadillo J. Abietane diterpenoids from *Salvia pachyphylla* and *S. clevelandii* with cytotoxic activity against human cancer cell lines. *J Nat Prod*. 2006;69:1803-05.
- Guterres SS, Alves MP, Pohlmann AR. Polymeric nanoparticles, nanospheres and nanocapsules, for cutaneous applications. *Drug Target Insights*. 2007;2:147-57.
- Guzman LA, Labhasetwar V, Song C, Jang Y, Lincoff AM, Levy R, Topol EJ. Local intraluminal infusion of biodegradable polymeric nanoparticles. A novel approach for prolonged drug delivery after balloon angioplasty. *Circulation*. 1996;94:1441-8.
- Hamdy S, Haddadi A, Shayeganpour A, Samuel J, Lavasanifar A. Activation of antigen-specific T cell-responses by mannan-decorated PLGA nanoparticles. *Pharm Res*. 2011;9:2288-301.
- Han J, Zhao D, Li D, Wang X, Jin Z, Zhao K, 2018 Jan 2 .Polymer-based nanomaterials and applications for vaccines and drugs. *Polymers*. 2018;10:31.

- Hanlon DJ, Aldo PB, Devine L, Alvero AB, Engberg AK, Edelson R, Mor G. Enhanced stimulation of anti-ovarian cancer CD8(+) T cells by dendritic cells loaded with nanoparticle encapsulated tumor antigen. *Am J Reprod Immunol.* 2011;65:597-609.
- Hans ML, Lowman AM. Biodegradable nanoparticles for drug delivery and targeting. *Curr Opin Solid State Mater Sci.* 2002;6:319-27.
- Harach T, Aprikian O, Monnard I, Moulin J, Membrez M, Beolor JC, Raab T, Mace K, Darimont C. Rosemary (*Rosmarinus officinalis* L.) leaf extract limits weight gain and liver steatosis in mice fed a high-fat diet. *Planta Med.* 2010;76:566-71.
- Hardwick JP, Osei-Hyiaman D, Wiland H, Abdelmegeed MA, Song BJ. PPAR/RXR regulation of fatty acid metabolism and fatty acid omega-hydroxylase (CYP4) isozymes: implications for prevention of lipotoxicity in fatty liver disease. *PPAR Res.* 2009;2009:9527-34.
- Hernández-Hernández E, Ponce-Alquicira E, Jaramillo-Flores ME, Guerrero Legarreta I. Antioxidant effect rosemary (*Rosmarinus officinalis* L.) and oregano (*Origanum vulgare* L.) extracts on TBARS and colour of model raw pork batters. *Meat Sci.* 2009;81:410-17.
- Hetal T, Bindesh P, Sneha T. Review on techniques for oral bioavailability enhancement of drugs. *Int J Pharm Sci Rev Res.* 2010;4:033.
- Hu J, Johnston KP, Williams RO 3RD. Nanoparticle engineering processes for enhancing the dissolution rates of poorly water soluble drugs. *Drug Dev Ind Pharm.* 2004;30:233-45.
- Ignea C, Athanasakoglou A, Ioannou E, Georgantea P, Triikka FA, Loupassaki S, Roussis V, Makris AM, Kampranis SC. Carnosic acid biosynthesis elucidated by a synthetic biology platform. *Proc Natl Acad Sci U S A.* 2016;113:3681-6.
- Jain RK, Stylianopoulos T. Delivering nanomedicine to solid tumors. *Nat Rev Clin Oncol.* 2010;7:653–64.
- Jaiswal J, Gupta SK, Kreuter J. Preparation of biodegradable cyclosporine nanoparticles by high-pressure emulsification solvent evaporation process. *J Control Release.* 2004;96:169-78.
- Jandus C, Simon HU, von Gunten S. Targeting siglecs-a novel pharmacological strategy for immuno- and glycotherapy, *Biochem. Pharmacol.* 2011;82:323-32.

- Jayasinghe C, Gotoh N, Aoki T, Wada S. Phenolics composition and antioxidant activity of sweet basil (*Ocimum basilicum* L.). *J Agric Food Chem*. 2003;51:4442-9.
- Jia L. Nanoparticle formulation increases oral bioavailability of poorly soluble drugs: approaches experimental evidences and theory. *Curr Nanosci*. 2005;1:237-43.
- Jiang T, Singh B, Li HS, Kim YK, Kang SK, Nah JW, Choi YJ, Cho CS. Targeted oral delivery of BmpB vaccine using porous PLGA microparticles coated with M cell homing peptide-coupled chitosan. *Biomaterials*. 2014;35:2365-73.
- Joshi MD1, Unger WW, van Beelen AJ, Bruijns SC, Litjens M, van Bloois L, Kalay H, van Kooyk Y, Storm G. DC-SIGN mediated antigen-targeting using glycan-modified liposomes: formulation considerations. *Int J Pharm*. 2011;2:426-32.
- Kalepu S, Nekkanti V. Insoluble drug delivery strategies: review of recent advances and business prospects. *Acta Pharm Sin B*. 2015;5:442-53.
- Kamaly N, Yameen B, Wu J, Farokhzad OC. Degradable controlled-release polymers and polymeric nanoparticles: mechanisms of controlling drug release. *Chem Rev*. 2016;116:2602-63.
- Karimi M, Solati N, Amiri M, Mirshekari H, Mohamed E, Taheri M, Hashemkhani M, Saeidi A, Estiar MA, Kiani P, Ghasemi A, Basri SM, Aref AR, Hamblin MR. Carbon nanotubes part I: preparation of a novel and versatile drug-delivery vehicle. *Expert Opin Drug Deliv*. 2015;12:1071-87.
- Karin S, Waldemar T. Antioxidative constituents of *Rosmarinus officinalis* and *Salvia officinalis*. *Z Lebensm Unters Forsch*. 1992;195:99-103.
- Kim YJ, Kim JS, Seo YR, Park JH, Choi MS, Sung MK. Carnosic acid suppresses colon tumor formation in association with antiadipogenic activity. *Mol Nutr Food Res*. 2014;58 2274-85.
- Kumar PS, Ramakrishna S, Saini TR, Diwan PV. Influence of microencapsulation method and peptide loading on formulation of poly(lactide-co-glycolide) insulin nanoparticles. *Pharmazie*. 2006;61:613-7.
- Kumar PS, Saini TR, Chandrasekar D, Yellepeddi VK, Ramakrishna S, Diwan PV Novel approach for delivery of insulin loaded poly(lactide-co-glycolide) nanoparticles using a combination of stabilizers. *Drug Deliv*. 2007;14:517-23.
- Kumari A, Yadav SK, Yadav SC. Biodegradable polymeric nanoparticles based drug delivery systems. *Colloids Surf B Biointerfaces*. 2010;75:1-18.

- Kwon H, Lee J, Song R, Hwang SI, Lee J, Kim YH, Lee HJ. In vitro and in vivo imaging of prostate cancer angiogenesis using anti-vascular endothelial growth factor receptor 2 antibody-conjugated quantum dot. *Korean J Radiol.* 2013;14:30-7.
- Last JA, Russell P, Nealey PF, Murphy CJ. The applications of atomic force microscopy to vision science. *Invest Ophthalmol Vis Sci.* 2010;51:6083-94.
- Linde H. Einneues Diterpenaus *Salvia officinalis* L. und eine Notizzur Konstitution von Pikrosalvin. *Helv. Chim. Acta.* 1964;47:1234-39.
- Liu G, Shen Y, Atreya HA, Parish D, Shao Y, Sukumaran DK, Xiao R, Yee A, Lemak A, Bhattacharya A, Acton TA, Arrowsmith CH, Montelione GT, Szyperski T. NMR data collection and analysis protocol for high-throughput protein structure determination. *PNAS.* 2005;102:10487-92.
- Liu H, Tu L, Zhou Y, Dang Z, Wang L, Du J, Feng J, Hu K. Improved Bioavailability and antitumor effect of docetaxel by TPGS modified proniosomes: *in vitro* and *in vivo* evaluations. *Sci Rep.* 2017;7:43372.
- Lu G, Haes AJ, Forbes TZ. Detection and identification of solids, surfaces, and solutions of uranium using vibrational spectroscopy. *Coord Chem Rev.* 2018;374:314-44.
- Lü JM, Wang X, Marin-Muller C, Wang H, Lin PH, Yao Q, Chen C. Current advances in research and clinical applications of PLGA-based nanotechnology. *Expert Rev Mol Diagn.* 2009;9:325-41.
- Luis JC, Johnson B. Seasonal variations of rosmarinic and carnosic acids in rosemary extracts. Analysis of their *in vitro* antiradical activity. *Span. J. Agric. Res.* 2005;3:106-12.
- Luo Y, Chen D, Ren L, Zhao X, Qin J. Solid lipid nanoparticles for enhancing vinpocetine's oral bioavailability. *J Control Release.* 2006;114:53-9.
- Macho Fernandez E, Chang J, Fontaine J, Bialecki E, Rodriguez F, Werkmeister E, Krieger V, Ehret C, Heurtault B, Fournel S, Frisch B, Betbeder D, Faveeuw C, Trottein F. Activation of invariant natural killer T lymphocytes in response to the α -galactosylceramide analogue KRN7000 encapsulated in PLGA-based nanoparticles and microparticles. *Int J Pharm.* 2012;423:45-54.
- Magenhein B, Levy MY, Benita S. A new *in vitro* technique for the evaluation of drug release profile from colloidal carriers-ultrafiltration technique at low pressure. *Int J Pharm.* 1993;94:115-23.

- Makadia HK, Siegel SJ. Poly lactic-co-glycolic acid (PLGA) as biodegradable controlled drug delivery carrier. *Polymers*. 2011;3:1377-97.
- Mandal A, Bisht R, Rupenthal ID, Mitra AK. Polymeric micelles for ocular drug delivery: From structural frameworks to recent preclinical studies. *J Control Release*. 2017;248:96-116.
- Manjunath K, Venkateswarlu V. Pharmacokinetics, tissue distribution and bioavailability of clozapine solid lipid nanoparticles after intravenous and intraduodenal administration. *J Control Release*. 2005;107:215-28.
- McDevitt MR, Chattopadhyay D, Kappel BJ, Jaggi JS, Schiffman SR, Antczak C, Njardarson JT, Brentjens R, Scheinberg DA. Tumor targeting with antibody-functionalized, radiolabeled carbon nanotubes. *J Nucl Med*. 2007;48:1180-90.
- McGill D, Chekmeneva E, Lindon JC, Takats Z, Nicholson JK. Application of novel solid phase extraction-NMR protocols for metabolic profiling of human urine. *Faraday Discuss*. 2019. doi:10.1039/c8fd00220g.
- Molavi, O., A. Mahmud, S. Hamdy, R.W. Hung, R. Lai, J. Samuel, A. Lavasanifar, Development of a poly(D, L-lactic-co-glycolic acid) nanoparticle formulation of STAT3 inhibitor JSI-124: implication for cancer immunotherapy. *Mol Pharm*. 2010;7:364-74.
- Molpeceres J, Aberturas MR, Guzman M. Biodegradable nanoparticles as a delivery system for cyclosporine: preparation and characterization. *J Microencapsul*. 2000;17:599-614.
- Morales-Cruz M, Flores-Fernández GM, Morales-Cruz M, Orellano EA, Rodríguez-Martínez JA, Ruiz M, Griebenow K. Two-step nanoprecipitation for the production of protein-loaded PLGA nanospheres. *Results Pharma Sci*. 2012;2:79-85.
- Morán L, Andrés S, Bodas R, Prieto N, Giráldez FJ. Meat texture and antioxidant status are improved when carnosic acid is included in the diet of fattening lambs. *Meat Sci*. 2012;91:430-4.
- Moreno S, Scheyer T, Romano CS, Vojnov AA. Antioxidant and antimicrobial activities of rosemary extracts linked to their polyphenol composition. *Free Radic Res*. 2006;40:223-31.

- Morgen M, Bloom C, Beyerinck R, Bello A, Song W, Wilkinson K, Steenwyk R, Shamblin S. Polymeric nanoparticles for increased oral bioavailability and rapid absorption using celecoxib as a model of a low-solubility, high-permeability drug. *Pharm Res.* 2012;29:427-40.
- Nabekura T, Yamaki T, Hiroi T, Ueno K, Kitagawa S. Inhibition of anticancer drug efflux transporter P-glycoprotein by rosemary phytochemicals. *Pharmacol Res.* 2010;61:259-63.
- Nahar M, Dutta T, Murugesan S, Asthana A, Mishra D, Rajkumar V, Tare M, Saraf S, Jain NK. Functional polymeric nanoparticles: an efficient and promising tool for active delivery of bioactives. *Crit Rev Ther Drug Carrier Syst.* 2006;23:259-318.
- Nekkanti V, Pillai R, Venkateshwarlu V, Harisudhan T. Development and characterization of solid oral dosage form incorporating candesartan nanoparticles. *Pharm Dev Technol.* 2009;14:290-8.
- Neophytou CM, Constantinou C, Papageorgis P, Constantinou AI. D-alpha-tocopheryl polyethylene glycol succinate (TPGS) induces cell cycle arrest and apoptosis selectively in Survivin-overexpressing breast cancer cells. *Biochem Pharmacol.* 2014;89:31-42.
- Onoue S, Yamada S, Chan HK. Nanodrugs: pharmacokinetics and safety. *Int J Nanomedicine.* 2014;20:1025-37.
- Ozdal ZD, Sahmetlioglu E, Narin I, Cumaoglu A. Synthesis of gold and silver nanoparticles using flavonoid quercetin and their effects on lipopolysaccharide induced inflammatory response in microglial cells. *3 Biotech.* 2019;9:212.
- Pal SL, Jana U, Manna PK, Mohanta GP, Manavalan R. Nanoparticle: an overview of preparation and characterization. *J Appl Pharm Sci.* 2011;1:228-34.
- Pandit RS, Gaikwad SC, Agarkar GA, Gade AK, Rai M. Curcumin nanoparticles: physico-chemical fabrication and its in vitro efficacy against human pathogens. *3 Biotech.* 2015;5:991-7.
- Pangi Z, Beletsi A, Evangelatos K. PEG-ylated nanoparticles for biological and pharmaceutical application. *Adv Drug Del Rev.* 2003;24:403-19.

- Park MY, Mun ST. Dietary carnosis acid suppresses hepatic steatosis formation via regulation of hepatic fatty acid metabolism in high-fat diet-fed mice. *Nutr Re Pract.* 2013;7:294-301.
- Peltonen L, Aitta J, Hyvönen S, Karjalainen M, Hirvonen J. Improved entrapment efficiency of hydrophilic drug substance during nanoprecipitation of poly(l)lactide nanoparticles. *AAPS PharmSciTech.* 2009;5:E16.
- Pi F, Zhang H, Li H, Thiviyanathan V, Gorenstein DG, Sood AK, Guo P. RNA nanoparticles harboring annexin A2 aptamer can target ovarian cancer for tumor-specific doxorubicin delivery. *Nanomedicine.* 2017;13:1183-93.
- Polakovic M, Gorner T, Gref R, Dellacherie E. Lidocaine loaded biodegradable nanospheres. II. Modelling of drug release. *J Control Release.* 1999;60:169-77.
- Rajapaksa TE, Stover-Hamer M, Fernandez X, Eckelhoefer HA, Lo DD. Claudin 4-targeted protein incorporated into PLGA nanoparticles can mediate M cell targeted delivery. *J Control Release.* 2010;142:196-205.
- Reuter J, Jocher A, Hornstein S, Mönning JS, Schempp CM. Sage extract rich in phenolic diterpenes inhibits ultraviolet-induced erythema *in vivo*. *Planta Med.* 2007;73:1190-1.
- Romo-Vaquero M, Larrosa M, Yáñez-Gascón MJ, Issaly N, Flanagan J, Roller M, Tomás-Barberán FA, Espín JC, Garcia-Conesa MT. A rosemary extract enriched in carnosis acid improves circulating adipocytokines and modulates key metabolic sensors in lean Zucker rats: critical and contrasting differences in the obese genotype. *Mol Nutr Food Res.* 2014;58:942-53.
- Roy A, Singh MS, Upadhyay P, Bhaskar S. Combined chemo-immunotherapy as a prospective strategy to combat cancer: a nanoparticle based approach. *Mol Pharm.* 2010;7:1778-88.
- Saini R, Saini S, Sharma S. Nanotechnology: the future medicine. *J Cutan Aesthet Surg.* 2010;3:32-3.
- Salatin S, Barar J, Barzegar-Jalali M, Adibkia K, Kiafar F, Jelvehgari M. Development of a nanoprecipitation method for the entrapment of a very water soluble drug into Eudragit RL nanoparticles. *Res Pharm Sci.* 2017;12:1-14.

- Sawant RL, Hadawale SD, Dhikale GK, Bansode CA, Tajane PS. Spectrophotometric methods for simultaneous estimation of rabeprazole sodium and aceclofenac from the combined capsule dosage form. *Pharm Methods*. 2011;2:193-7.
- Schrap SM, Opperhuizen A. Relationship between bioavailability and hydrophobicity: reduction of the uptake of organic chemicals by fish due to the sorption on particles. *Environ Toxicol Chem*. 1990;9:715-24.
- Schwarz K, Ternes W. Antioxidative constituents of *Rosmarinus officinalis* and *Salvia officinalis*. II. isolation of carnosic acid and formation of other phenolic diterpenes. *Z Lebensm Unters Forsch*. 1992;195:99-103.
- Scott CJ, Marouf WM, Quinn DJ, Buick RJ, Orr SJ, Donnelly RF, McCarron PA. Immunocolloidal targeting of the endocytotic siglec-7 receptor using peripheral attachment of siglec-7 antibodies to poly(lactide-co-glycolide) nanoparticles. *Pharm Res*. 2008;25:135-46.
- Shan W, Gao L, Zeng W, Hu Y, Wang G, Li M, Zhou J, Ma X, Tian X, Yao J. Activation of the SIRT1/p66shc antiapoptosis pathway via carnosic acid induced inhibition of miR-34a protects rats against nonalcoholic fatty liver disease. *Cell Death Dis*. 2015;6:e1833.
- Shaw TK, Mandal D, Dey G, Pal MM, Paul P, Chakraborty S, Ali KA, Mukherjee B, Bandyopadhyay AK, Mandal M. Successful delivery of docetaxel to rat brain using experimentally developed nanoliposome: a treatment strategy for brain tumor. *Drug Deliv*. 2017;24:346-57.
- Singh R, Lillard JW Jr. Nanoparticle-based targeted drug delivery. *Exp Mol Pathol*. 2009;86:215-23.
- Sithole MN, Choonara YE, du Toit LC, Kumar P, Marimuthu T, Kondiah PPD, Pillay V. Development of a Novel Polymeric Nanocomposite Complex for Drugs with Low Bioavailability. *AAPS PharmSciTech*. 2018;19:303-14.
- Som C, Nowack B, Krug HF, Wick P. Toward the development of decision supporting tools that can be used for safe production and use of nanomaterials. *Acc Chem Res*. 2013;46:863-72.
- Stark JL, Hamid R, Eghbalnia , Lee W, Westler WM, Markley JL. NMRmix: a tool for the optimization of compound mixtures in 1D ¹H NMR ligand affinity screens. *J Proteome Res*. 2016;15:1360-8.

- Takeuchi H, Yamamoto Y. Mucoadhesive nanoparticulate system for peptide drug delivery. *Adv Drug Del Rev.* 2001;47:39-54.
- Tao W, Zeng X, Zhang J, Zhu H, Chang D, Zhang X, Gao Y, Tang J, Huang L, Mei L. Synthesis of cholic acid-core poly([varepsilon]-caprolactone-ranlactide)-b-poly(ethylene glycol) 1000 random copolymer as a chemotherapeutic nanocarrier for liver cancer treatment. *Biomater Sci.* 2014;2:1262-74.
- Torres-Ortega PV, Saludas L, Hanafy AS, Garbayo E, Blanco-Prieto MJ. Micro- and nanotechnology approaches to improve Parkinson's disease therapy. *J Control Release.* 2019;295:201-13.
- Uğurbil K. Imaging at ultrahigh magnetic fields: History, challenges, and solutions. *Neuroimage.* 2018;168:7-32.
- Vasir JK, Labhasetwar V. Quantification of the force of nanoparticle-cell membrane interactions and its influence on intracellular trafficking of nanoparticles. *Biomaterials.* 2008;29:4244-52.
- von GS, Bochner BS. Basic and clinical immunology of Siglecs, *Ann N Y Acad Sci.* 2008;1143:61-82.
- Wang Y, Tan Y. Enhanced drug loading capacity of 10-hydroxycamptothecin- loaded nanoparticles prepared by two-step nanoprecipitation method. *J. Drug Deliv. Sci. Technol.* 2016;36:183–91.
- Wei J, Bristow A, McBride E, Kilgour V, O'Connor PB. d- α -tocopheryl polyethylene glycol 1000 Succinate: a view from FTICR MS and Tandem MS. *Anal Chem.* 2014; 86: 1567-74.
- Wenkert E, Fuchs A, McChesney JD. Chemical artifacts from the family Labiatae. *J Org Chem.* 1965;30:2931-4.
- Wu JZ, Williams GR, Li HY, Wang D, Wu H, Li SD, Zhu LM. Glucose- and temperature-sensitive nanoparticles for insulin delivery. *Int J Nanomedicine.* 2017;12:4037-57.
- Xie J, VanAlstyne P, Uhlir A, Yang X. A review on rosemary as a natural antioxidation solution. *Eur J Lipid Sci Technol.* 2017;119:1600439.
- Yaguchi T, Sumimoto H, Kudo-Saito C, Tsukamoto N, Ueda R, Iwata-Kajihara T, Nishio H, Kawamura N, Kawakami Y. The mechanisms of cancer immunoescape and development of overcoming strategies. *Int J Hematol.* 2011;93:294-300.

- Yan H, Wang L, Li X, Yu C, Zhang K, Jiang Y, Wu L, Lu W, Tu P. High-performance liquid chromatography method for determination of carnosic acid in rat plasma and its application to pharmacokinetic study. *Biomed Chromatogr.* 2009;23:776-81.
- Yan L, Gu Z, Zhao Y. Chemical mechanisms of the toxicological properties of nanomaterials: generation of intracellular reactive oxygen species. *Chem Asian J.* 2013;8:2342-53.
- Yang C, Wu T, Qi Y, Zhang Z. Recent advances in the application of vitamin E TPGS for drug delivery. *Theranostics.* 2018;8:464-85.
- Yavuz B, Pehlivan SB, Unlü N. Dendrimeric systems and their applications in ocular drug delivery. *Sci World J.* 2013;2013:7323-40.
- Zhang W, Wang C, Li Z, Lu Z, Li Y, Yin JJ, Zhou YT, Gao X, Fang Y, Nie G, Zhao Y. Unraveling stress-induced toxicity properties of graphene oxide and the underlying mechanism. *Adv Mater.* 2012;24:5391-7.
- Zhang Z, Tongchusak S, Mizukami Y, Kang YJ, Ioji T, Touma M, Reinhold B, Keskin DB, Reinherz EL, Sasada T. Induction of anti-tumor cytotoxic T cell responses through PLGA-nanoparticle mediated antigen delivery. *Biomaterials.* 2011;32:
- Zhu G, Mallery SR, Schwendeman SP. Stabilization of proteins encapsulated in injectable poly (lactide- co-glycolide). *Nat Biotechnol.* 2000;18:52-7.
- Zhu H, Chen H, Zeng X, Wang Z, Zhang X, Wu Y, Gao Y, Zhang J, Liu K, Liu R, Cai L, Mei L, Feng SS. Co-delivery of chemotherapeutic drugs with vitamin E TPGS by porous PLGA nanoparticles for enhanced chemotherapy against multi-drug resistance. *Biomaterials.* 2014;35:2391-400.